Faculty of Bioscience Engineering
Academic year 2014-2015

Foliar water uptake and its link to growth in *Avicennia marina* (Forskk.) Vierh.

Jeroen Schreel

Promoter: Prof. dr. ir. Kathy Steppe

Tutor: Prof. dr. ir. Kathy Steppe
ir. Bart Van de Wal

Master thesis submitted to obtain the degree of
Master of Science in Bioscience Engineering: Forest and Nature Management

The author and promoter give the permission to use this thesis for consultation and to copy parts of it for personal use. Every other use is subject to the copyright laws, more specifically the source must be extensively specified when using results from this thesis.

De auteur en promotor geven de toelating dit eindwerk te consulteren en delen ervan te kopiëren voor persoonlijk gebruik. Elk ander gebruik valt onder de beperkingen van het auteursrecht, in het bijzonder met betrekking tot de verplichting uitdrukkelijk de bron te vermelden bij het aanhalen van resultaten uit dit eindwerk.

Gent, juni 2015

The promoter
Prof. dr. ir. Kathy Steppe

The tutor
ir. Bart Van de Wal

The author
Jeroen Schreel

Acknowledgment

'Kennis is een rijkdom die ze niet kunnen afnemen'

(Maurice Vermeulen)

Nu mijn traject als student op zijn einde loopt en de laatste hand wordt gelegd aan deze thesis zijn er enkele mensen die ik graag zou willen bedanken.

Als eerste zijn er mijn ouders. Ondanks de vele 'ups' en 'downs' hebben ze mij altijd gesteund. Ze wisten hoe graag ik deze richting wou volgen en dat was voldoende. Daarvoor heel erg veel dank. Ten tweede zijn er mijn zus en neefje, Lien en Elewa. Dit laatste jaar bracht ik hen wekelijks een bezoekje, met het doel hen wat te helpen. Ik kan echter oprecht zeggen dat zij mij veel meer geholpen hebben dan ik hen. Daarvoor heel erg veel dank. Ten derde zijn er mijn grootouders. Ook zij bleven mij steunen in alle mogelijke opzichten. Ik werd dan ook regelmatig verwend met lekkere soep, koekjes en snoepjes. Tot mijn grote spijt mag één van hen het einde van mijn studies niet meer meemaken. Mijn opa was een waar voorbeeld. Hij kon meepraten over mijn studies en gaf interessante inzichten. Zijn levensvreugde en genot van de kleine dingen was fenomenaal en inspirerend. Opa, je bent heen gegaan maar niet vergeten. Je zal altijd een bron van inspiratie voor mij blijven. Bedankt. Ten vierde is er mijn vriendin, Shari. Je begrijpt mij, geeft mij tijd en ruimte als ik het nodig heb en bent er voor mij. Ik kan met zekerheid zeggen dat ik deze thesis nooit zo "rustig" zou kunnen hebben afgelegd zonder jou. Bij deze wil ik je hier ook oprecht voor bedanken.

Vervolgens zijn er de leiding en de medewerkers van het labo. Mijn promotor Prof. dr. ir. Kathy Steppe wil ik heel erg bedanken voor haar begeleiding en enthousiasme. Ondanks haar heel erg drukke agenda trachtte ze steeds tijd voor mij vrij te maken als dit nodig was. Ik mocht eerlijk mijn mening geven en voelde mij daardoor meteen thuis. Eveneens mijn tutor ir. Bart Van de Wal wil ik heel erg bedanken. Hij was steeds bereid mij te helpen met mogelijke problemen en heeft me alle berekeningen en methodes adequaat en zorgvuldig uitgelegd. Tenslotte zijn er nog de technici: Geert Favyts, Philip Deman, Erik Moerman en Thomas Van De Putte. Hen wil ik hartelijk danken voor alle technisch en praktische hulp gedurende dit hele thesis-avontuur. Zonder hun hulp was ik waarschijnlijk

verdronken in de wereld van data-logging.

Last but not least I want to thank Pedro Hervé Fernández. Thanks to his proper guidance and planning we were able to conduct the deuterium experiments. He was always prepared to help and has a, for me previously unknown, positive energy in everything he does. For this enrichment, thank you.

Jeroen Schreel,
Gent, juni 2015

Abstract

Mangrove ecosystems are well adapted to the intertidal zones between land and sea of tropical and subtropical coastal areas. The salinity occurring in these environments might induce a state of physiological drought. Mangroves, however, have some specific adaptations to survive in this saline environment such as the exclusion of salt at the root level, the use of salt glands at the leaf level and the accumulation of high intracellular osmotic compound concentrations in leaves and roots. Upcoming climate change might make it more difficult for mangrove species to survive and grow. On the other hand, foliar water uptake during precipitation events might mitigate the effects of these changes.

In this thesis work the ability of foliar water uptake by *Avicennia marina* and its link to growth for this species were explored. Several ecophysiological variables were measured such as sap flow, stem diameter variations and leaf water potentials prior, during and post artificial rain events. Hydraulic redistribution and abiotic parameters such as air temperature and relative humidity were recorded as well. Based on the air temperature and the relative humidity, the vapor pressure deficit was calculated. All experiments took place in the controlled setting of a greenhouse.

We investigated the possibility of foliar water uptake through submergence of leaves and leaf water potential measurements. The leaf water content of submerged young leaves increased indicating foliar water uptake. During artificial rain events the leaf water potential increased to a value similar to the water potential of the irrigation water, indicating a hydraulic equilibrium. To assess the hydraulic redistribution imposed by this hydraulic equilibrium an artificial rain event with deuterated water was performed. This experiment proved that water was taken up by the leaves and redistributed to other plant organs. The first organs that were replenished were organs close to the point of uptake, in this case the leaves. Concomitant with the artificial rain events, a negative sap flow and an increase in stem diameter were measured. The negative sap flow confirmed that water was taken up by the leaves and redistributed to other plant organs. The diameter increase during artificial rain events was substantial and indicated that growth occurred due to these events. Over a two-day period saplings showed an average increase in diameter of 0.03 $mm.day^{-1}$ during artificial rain events, compared to an average increment in diameter of 0.01 $mm.day^{-1}$ when no artificial rain events occurred. In addition, no large decreases in stem diameter were observed during the whole experiment, indicating that the increase

resulting from foliar water uptake was permanent. No large increment in diameter was measured in the absence of an artificial rain events, suggesting that freshwater supplied by these events is crucial in order to induce and maintain a significant permanent growth for *Avicennia marina*.

Keywords: foliar water uptake, *Avicennia marina*, mangroves, climate change, sap flow, stem diameter variations, stable isotopes

Samenvatting

Mangrove-ecosystemen zijn goed aangepast aan de getijdenzones tussen land en zee van tropische en subtropische kusten. Het hoge zoutgehalte in deze omgevingen kan een toestand van fysiologische droogte induceren. Mangroves hebben echter een aantal specifieke aanpassingen om te overleven in deze zoute omgeving zoals de uitsluiting van zout op het wortelniveau, het gebruik van zoutklieren op het bladniveau en de accumulatie van hoge intracellulaire concentraties aan osmotische stoffen in de bladeren en wortels. Met de opkomende klimaatverandering kunnen mangrovesoorten het moeilijker hebben om te overleven en te groeien. Blad-wateropname tijdens neerslag gebeurtenissen kunnen de weerslag van deze veranderingen verzachten.

In dit artikel werd de mogelijkheid van blad-wateropname door *Avicennia marina* en de link met de groei voor deze soort onderzocht. Verschillende ecofysiologische variabelen werden gemeten zoals sapstroom, stam diameter variaties en blad-waterpotentialen voor, tijdens en na kunstmatige beregening. Hydraulische herverdeling en abiotische parameters zoals luchttemperatuur en relatieve vochtigheid werden ook opgemeten. Op basis van de temperatuur en de relatieve vochtigheid, werd het dampdrukdeficiet berekend. Alle experimenten vonden plaats onder gecontroleerde omstandigheden in een serre.

We onderzochten de mogelijkheid van blad-wateropname door de onderdompeling van bladeren, en met behulp van blad-waterpotentiaal metingen. Het blad-watergehalte van ondergedompelde jonge bladeren nam toe en toonde aan dat blad-wateropname plaatsvond. Tijdens kunstmatige beregening steeg de blad-waterpotentiaal tot een vergelijkbare waarde als de waterpotentiaal van het irrigatiewater, wat een hydraulisch evenwicht indiceert. Om de hydraulische herverdeling door dit hydraulisch evenwicht te bepalen, werd een kunstmatige beregening met gedeutereerd water uitgevoerd. Dit experiment bewees dat water werd opgenomen door de bladeren en herverdeeld naar andere plantorganen. De eerste organen die werden aangevuld waren organen dicht bij het punt van opname, in casu de bladeren. Gelijktijdig met de kunstmatige beregening, werd een negatieve sapstroom en een toename in stam diameter gemeten. De negatieve sapstroom bevestigt dat het water werd opgenomen door de bladeren en herverdeeld naar andere plantorganen. De toename van de diameter tijdens kunstmatige beregening was aanzienlijk en gaf aan dat groei zich voordeed als gevolg van deze behandeling. Over een tweedaagse periode vertoonden de jonge boompjes een gemiddelde diametertoename van $0,03\ mm.dag^{-1}$ bij de aanwezigheid

van kunstmatige beregening, vergeleken met een gemiddelde toename in diameter van $0,01$ $mm.dag^{-1}$ als er geen kunstmatige beregening plaatsvond. Bovendien werden geen grote afnames in stam diameter waargenomen tijdens het volledige experiment, wat aangeeft dat de toename als gevolg van blad water opname permanent was. Er werd ook geen grote toename in diameter gemeten in afwezigheid van een kunstmatige beregening, wat suggereert dat het toegediende zoetwater essentieel is om een aanzienlijke blijvende groei bij *Avicennia marina* te veroorzaken en handhaven.

Trefwoorden: blad-wateropname, *Avicennia marina*, mangroves, klimaatsverandering, sapstroom, stam diameter variaties, stabiele isotopen

List of Symbols and Abbreviations

Abbreviations

Abbreviation	In full	Unit
ABA	Abscisic acid	–
DOY	Day Of Year	–
FWU	Foliar Water Uptake	$m.s^{-1}$
HD	Hydraulic Descent	–
HFD	Heat Field Deformation method	–
HHR	Horizontal Hydraulic Redistribution	–
HL	Hydraulic Lift	–
HR	Hydraulic Redistribution	–
LAI	Leaf Area Index	$m^2_{leaves}.m^{-2}_{soil}$
LVDT	Linear Variable Displacement Transducer	–
LWC	Leaf Water Content	%
NTC	Negative Temperature Coefficient	–
PAR	Photosynthetically Active Radiation	$\mu mol.m^{-2}s^{-1}$
RC	Resistance-Capacitance	–
RCP	Representative Concentration Pathways	–
RH	Relative Humidity	%
RSF	Relative Sap Flow; HFD-ratio	–
RSF_s	Simplified Relative Sap Flow; Simplified HFD-ratio	–
SDV	Stem Diameter Variation	μm
SF	Sap flow	$g.h^{-1}$
SFD	Sap-flux density	$g.cm^{-2}.h^{-1}$
SMD	Surface-Mounted Device	–
SPAC	Soil-Plant-Atmosphere Continuum	–
SWU	Stem Water Uptake	$m.s^{-1}$
TD	Tissue Dehydration	–
VHR	Vertical Hydraulic Redistribution	–
VPD	Vapor Pressure Deficit	kPa

Symbols

Roman symbols

Symbol	Description	Unit
C	Capacitance	$mg.MPa^{-1}$
C_o	Osmolality	$mol.l^{-1}$
D	Thermal diffusivity	$cm^2.s^{-1}$
δD	Deuterium isotope composition	‰ ; $g.kg^{-1}$
E	Transpiration rate	$g.h^{-1}$
e_o	Actual vapor pressure	kPa
e_o^v	Saturated vapor pressure	kPa
f	Sap flow between xylem and storage compartment	$mg.s^{-1}$
g	Gravitational acceleration	$m.s^{-2}$
g_s	Stomatal conductance	$mmol.m^{-2}.s^{-1}$
h	Height	m
$k_{source-sink}$	Efficiency of transport from source to sink	$m.s^{-1}.MPa^{-1}$
L_{sw}	Measuring depth into the sapwood	cm
N	Percentage of water originating from FWU of deuterated water	%
Q	The number of plant parts in the respective sample	–
R	Hydraulic resistance	$MPa.h.g^{-1}$
R_g	Gas constant	$J.mol^{-1}.K^{-1}$
R_{sample}	Deuterium over hydrogen ratio of sample	–
$R_{standard}$	Deuterium over hydrogen ratio of standard	–
T	Temperature	K or $°C$ (indicated)
T_{air}	Air temperature	$°C$
T_{leaf}	Leaf temperature	$°C$
dT_{as}	Temperature difference between lower and tangential needle	K
dT_{s-a}	Temperature difference between upper and tangential needle	K
$dT0_{s-a}$	Temperature difference between upper and tangential needle during zero flow	K
dT_{sym}	Temperature difference between upper and lower needle	K
V	Volume	m^3
W	Water content	mg
Z_{ax}	Axial distance between upper/lower needle and heater	cm
Z_{tg}	Distance between tangential needle and heater	cm

Greek symbols

Symbol	Description	Unit
Γ	Critical value for the pressure component which must be exceeded for producing growth	MPa
ρ_b	Density of wood	$kg.m^{-3}$
ρ_w	Density of water	$kg.m^{-3}$
ϕ	Cell wall extensibility	$MPa^{-1}.s^{-1}$
Ψ	Total water potential	MPa
$\Delta\Psi$	Difference in total water potential	MPa
$\Delta\Psi_{source-sink}$	Difference in total water potential between source and sink	MPa
Ψ_g	Gravity potential	MPa
Ψ_{leaf}	Water potential of leaf	MPa
Ψ_m	Matrix potential	MPa
Ψ_o	Osmotic water potential	MPa
Ψ_p	Hydrostatic water potential	MPa
Ψ_{root}	Water potential of root	MPa
Ψ_{soil}	Water potential of soil	MPa

Contents

Introduction

In contrast to their low terrestrial coverage, a significant amount of communities are dependent on mangrove ecosystems for their survival. One of the most common and predominant species in the mangrove forests is *Avicennia marina* (Forskk.) Vierh. However, due to climate change, precipitation patterns will shift resulting in a different input of freshwater for these areas. Even more, sea-levels will rise pushing back these ecosystems and causing a rise in salinity (IPCC, 2014). How will *A. marina* cope? Will the anthropogenic communities be able to depend on these ecosystems in the future or will they have to look for alternatives or even move to meet their needs of firewood, construction wood and food?

A hypothesis has been put forward stating that *A. marina* could benefit from precipitation by foliar water uptake and thus could maintain growth in what would otherwise be unfavorable conditions. Assuming that this hypothesis is valid also implies benefits from an increase in precipitation.

In order to confirm this hypothesis first a literature review has been conducted. This chapter will commence with a short discussion of mangroves in general in order to generate a better understanding of these ecosystems. Secondly the parameters of climate change affecting this hypothesis are briefly discussed. Finally water relations in the soil-plant-atmosphere continuum resulting in sap flow and hydraulic redistribution patterns like foliar water uptake will conclude this chapter.

The second chapter will deal with material and methods and will discuss how this research was conducted. This chapter will be followed by a third chapter illustrating the results of the conducted measurements. A subsequent chapter will deal with a more in depth discussion of the former mentioned results. In the last chapter a general conclusion will be given.

Chapter 1

Literature review

1.1 Mangrove forests and their distribution

Mangroves are a diverse group of evergreen trees, shrubs and ferns growing in the intertidal zone between land and sea along tropical and subtropical coastlines (Clough, 2013) (Figure 1.1). This latitudinal distribution of mangroves coincides with the geographical limits of arid regions. These findings suggest that the distribution of mangrove communities is more limited by rainfall and aridity than by air temperature (Spalding et al., 1997; Clough, 2013). However, Hogarth (2007) stated that mangrove distribution is closely correlated with sea temperature. Therefore, a temperature dependence cannot be excluded. In addition, more recent studies by Uddin et al. (2014) and Van de Wal et al. (2015) indicated the possibility of foliar water uptake (FWU) and changes in radial sap-flux density (SFD) patterns of *A. marina* during rain events, respectively, emphasizing the importance of precipitation. Santini et al. (2015) stated that precipitation correlated with higher growth and production rates due to a decrease in salinity. This might also be partly induced by FWU. Combining these findings raises questions about the resilience of this species and mangroves in general to changes in precipitation patterns under ongoing global change.

Overall mangroves may act as an important stabilizing factor for riverbanks and coastlines. Their presence may also reduce flooding of more landward areas. Nevertheless, because of the specific growing conditions in these areas, species composition is rather limited (Polidoro et al., 2010). However, the growing population density, and as a consequence increasing needs of building materials, firewood, charcoal, food and medicine or industrial and urban development, competes for the use of mangrove ecosystems. As a consequence pressure on these few species has increased dramatically leading to significant loss of mangrove resources (Spalding et al., 1997; Polidoro et al., 2010). Examples include the conversion of mangrove habitats to palm plantations in Malaysia and Indonesia, to rice fields in Western Africa and the Philippines and to shrimp ponds in Asia and Latin America (Clough, 2013). Nonetheless, species composition in a specific mangrove community is not only anthropologically driven but is also dependent on the duration, depth and

periodicity of flooding with salt water, the salinity of this water and the compound and structure of the substrate in general (Cardona-Olarte et al., 2013; Mitra, 2013).

Figure 1.1: Worldwide distribution of mangrove forests indicated in green (Giri et al., 2011).

Saline environments induce physiological drought in plants, making water acquisition more energetically unfavorable than in non-saline conditions (Reef & Lovelock, 2014). Due to this harsh ecological environment, mangrove species have developed three basic mechanisms in order to cope with high salinity. First there are salt excluders which exclude salt by an ultra filtration method at the root level called 'reverse osmosis' (Mitra, 2013). In order to keep an osmotic balance, salt excluders need to actively produce organic components. This process consumes energy and is mainly used by species growing in a low salinity (Lüttge, 2008). Second there are salt includers or accumulators which accumulate salt in their leaves. This salt can be accumulated intracellular or compartmentalized. Subsequently, these species can either defoliate to reduce excess salt or maintain their leaves which have a negative water potential in order to draw water through the soil-plant-atmosphere continuum (SPAC) (Lüttge, 2008; Mitra, 2013) (section 1.4). Third there are salt excreters. These species excrete excess salt, taken up through their roots, through salt glands at the leaf level (Lüttge, 2008; Mitra, 2013). Subsequent events like washing or blowing away of salt by precipitation or wind, respectively, occur regularly (Tomlinson, 1986). Lüttge (2008) states however that the distinction between salt excluders and salt includers is relative as there is always some control of salt uptake at the root level, i.e. *A. marina* is an excluder with salt glands, which can also accumulate salt internally. To some extend all three mechanisms can be utilized by the same species. As Hogarth (2007) stated (p. 19): *'Exclusion, tolerance, and secretion are used with different emphasis by different species, and within a species under different environmental conditions.'*

1.2 Ecophysiology of *Avicennia marina*

A. marina has a very wide distribution pattern (Figure 1.2). This pattern includes about half of the terrestrial tropics. The cause of this widespread distribution lies in several factors such as a considerable tolerance to variations in water salinity and the ability to cope with extreme temperature conditions. They can withstand some degree of frost due to very small xylem vessel diameters, which prevent cavitation, and tolerate long submergence of their pneumatophores during exceptional floods (Spalding et al., 1997).

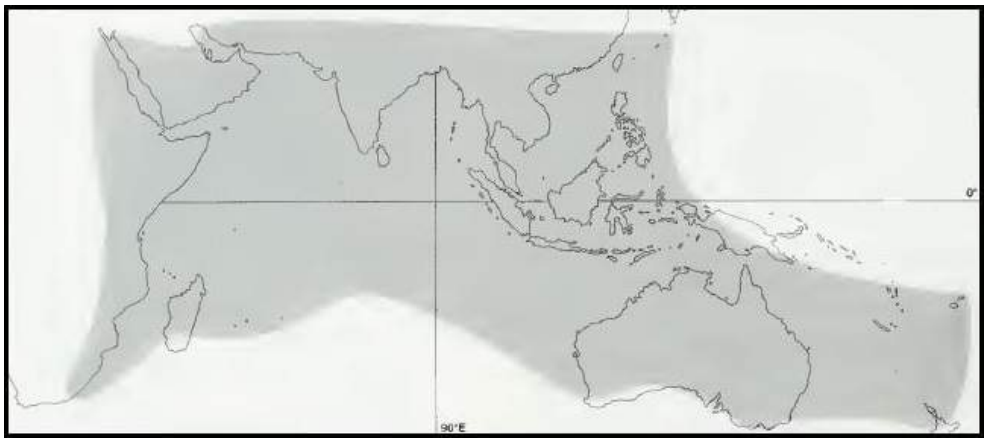

Figure 1.2: Distribution area of *Avicennia marina* indicated in gray (Spalding et al., 1997).

Although there have been speculations about the low transpiration rate of mangroves, it has been reported that transpiration of *Avicennia* species is high in comparison to other mangrove species (Becker et al., 1997). In addition, the *Acanthaceae* family has been known for its tolerance to hyper saline conditions. The distinct tolerance of *Avicennia* spp. to salinity lies in different functional mechanisms such as the exclusion of salt at the root level, the use of salt glands (Figure 1.3) and the accumulation of high intracellular inorganic ion concentrations in leaves and roots (Suárez et al., 1998) thus lowering the osmotic water potential (Ψ_o) (subsection 1.4.1). Important is that leaf features such as salt gland density can vary significantly according to salinity and shading (Tomlinson, 1986). Salt exclusion at root level is the most predominant feature for *Avicennia* spp. which excludes 90 to 97 % of salt in high salinity water (Hogarth, 2007). Within the salt glands ions are secreted by the secretory cells into the subcuticular space at the head of the gland. Water follows this flow passively creating a pressure in the subcuticular space, opening pores in the cuticle and releasing a solution with a high salinity (Lüttge, 2008). Notwithstanding these adaptations, it should be noted that a high salinity still substantially decreases leaf longevity for *A. marina* (Suárez et al., 1998), compared to the average leaf longevity oscillating between 9 and 11 months (Wang'ondu et al., 2010), and results in an increase in cuticle thickness (Reef & Lovelock, 2014).

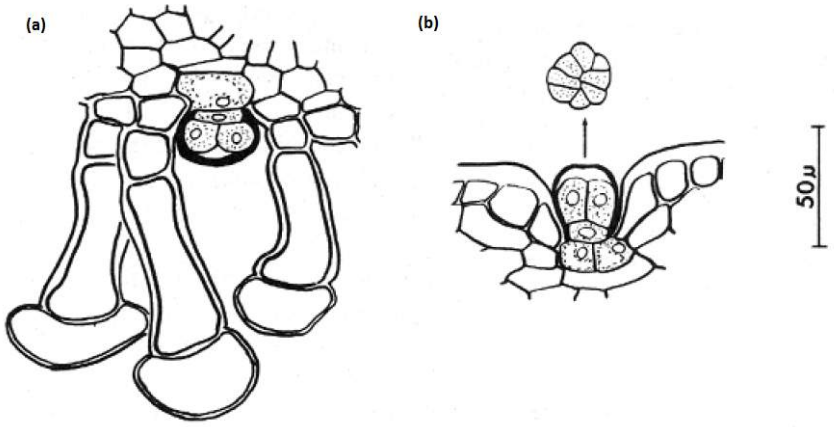

Figure 1.3: Salt glands of *Avicennia marina* (Tomlinson, 1986). (a) Abaxial salt gland, surrounded by non-glandular hairs. (b) Adaxial salt gland, scattered in individual shallow pits.

The rooting system of *Avicennia* species consists of several key elements (Figure 1.4). The basis is a cable root system that spreads radially from the mother tree. On these cable roots there are pneumatophores growing upwards which allow gas exchange through lenticels, and anchoring or support roots growing downward in the substrate which generates stability (Ong & Gong, 2013). Aboveground gas exchange is necessary due to a lack of oxygen by water logging and the need of oxygen at root level for respiration (Hogarth, 2007). The root epidermal cells contain suberin, a hydrophobic compound deposited between the cell wall and the plasma membrane. As such an effective barrier for passive ion and water transport is provided. In combination with the highly developed Casparian strip at the root endodermis, almost all apoplastic water is blocked (Reef & Lovelock, 2014).

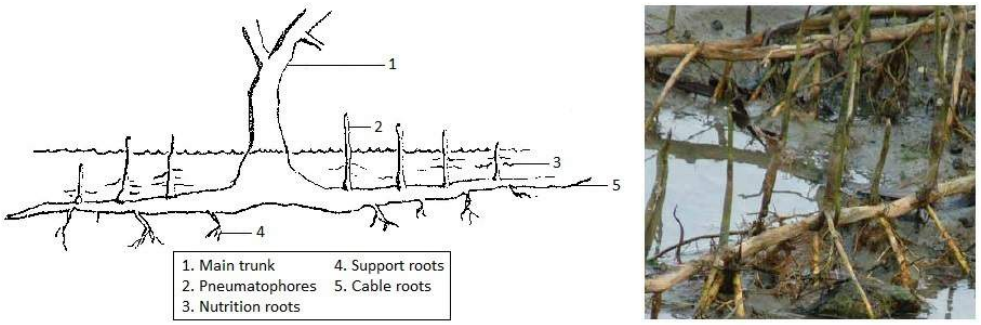

Figure 1.4: Left: Simplified diagram of the mature *Avicennia marina* rooting system (Crumbie, 1987). Right: Eroded substrate shows horizontal cable roots of *Avicennia marina* that spread radially from the parent tree with pneumatophores growing upward and support roots growing downward (Ong & Gong, 2013).

1.3 Climate change

Water movement within a classical terrestrial ecosystem consists of several inputs and outputs such as precipitation, transpiration and runoff as well as some internal transfers. Mangrove ecosystems are often water saturated. As a consequence, the water balance dynamics vary significantly in comparison to a classical terrestrial ecosystem. With climate change these dynamics will change and have their effect on the productivity and occurrence of mangrove ecosystems.

The vulnerability of ecosystems to climate change varies from region to region and even sub region to sub region. Understanding these variations and estimating their impact on different regions is essential in predicting the possible effects of global climate change. Only through this channel of focus, mitigation can truly take place in a responsible way.

It is important to note and keep in mind that changes in climate have several feedback loops e.g. the water vapor feedback loop and the snow albedo feedback loop (Chapin et al., 2002). These loops are out of the scope of this paper, but are implemented implicitly in the models used to predict climate change.

1.3.1 Precipitation

Notwithstanding the importance of the intensity of precipitation, Biasutti & Yuter (2013) stated that most of the research on climate change and rainfall extremes is limited to the daily timescale, despite the expectation of more extreme precipitation events under global warming. Thus, the underlying problem manifests itself as follows: when e.g. 20 mm of precipitation is predicted for a one day measurement, will it fall in 30 minutes or 20 hours? Rainfall of 30 minutes might imply a dry day with a short wetting event, while rainfall of 20 hours implies a wet day with a high relative humidity (RH). The importance of this question cannot be overstated. However, due to limited research little is known about this variable, although several models have been constructed to access the current and expected total amounts and extremes of precipitation.

Total precipitation rates are predicted to increase drastically, while these changes will not be uniformly distributed around the globe. When overlaying Figure 1.5 with Figure 1.2 and Figure 1.1 it can be expected that mangroves containing *A. marina* in Asia will receive more precipitation, while mangroves in southern Africa will have a smaller rainfall input.

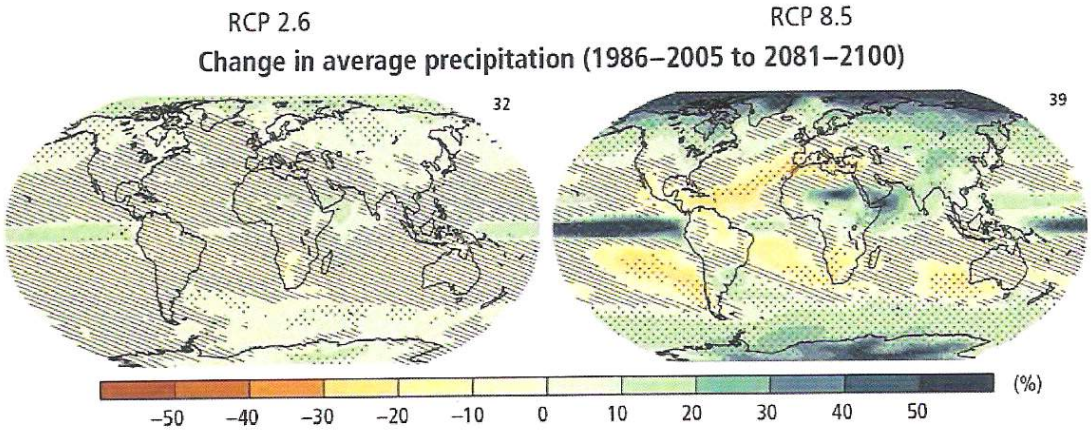

Figure 1.5: Change in average precipitation based on multi-model mean projections for 2081-2100 relative to 1986-2005 under the Representative Concentration Pathways (RCP) 2.6 (left) and RCP 8.5 (right) scenarios. The number of models used is indicated in the upper right corner of each panel. Dots show regions where the projected change is large compared to natural internal variability, and where at least 90 % of the models agree on the sign change. Diagonal lines show regions where projected change is less than one standard deviation of the natural internal variability (IPCC, 2014).

A decrease in precipitation may cause a significant increase in salinity which is likely to reduce productivity, growth and seedling survival favoring more salt-tolerant species. On the other hand an increase in precipitation may cause an increase in mangrove area, diversity and production due to the reduced salinity (Mitra, 2013). In general mangrove trees tend to be larger in regions with a higher amount of precipitation, suggesting a growth limitation more based on rainfall and aridity than temperature (Spalding et al., 1997; Vandegehuchte et al., 2014b), as mentioned earlier in section 1.1.

The conclusion can be made that changes in precipitation patterns are expected to affect mangrove growth parameters, and the distribution of mangrove ecosystems, by altering salinity levels of the aquatic phase (Mitra, 2013). However, if the hypothesis stated in the introduction is valid, the importance of precipitation is underestimated by only accounting for a change in salinity.

1.3.2 Salinity

Changes in precipitations patterns, or a sea-level rise, will alter the salinity in mangrove ecosystems. The intrusion of seawater in the upstream zones of estuaries due to a sea-level rise increases salinity in these areas while a higher amount of precipitation reduces salinity (section 1.3.1). A rise in sea-level has been observed for over 100 years (Figure 1.6), approximated by 19 cm in 2010 compared to 1900. An additional rise of approximately

40 to 70 cm over the next 100 years is expected, stressing the importance of sea-level rise and the concomitant rise in salinity for certain areas. Mitra (2013) stated that mangrove ecosystems cannot keep pace with the rate of sea-level rise. This raises questions about the possibility of assisted migration of mangrove forests. Assisted migration must be considered in order to preserve these ecosystems. The ecological and ethical implications of this strategy will not be discussed in this paper.

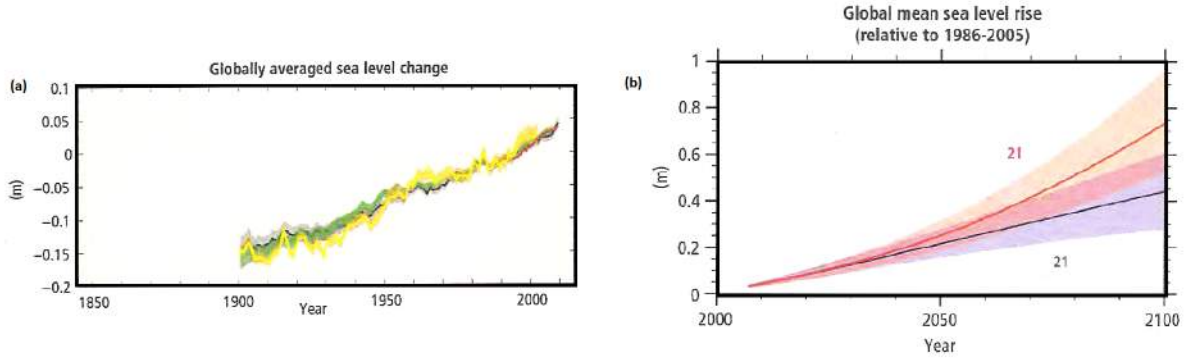

Figure 1.6: Global sea level change in past and future (IPCC, 2014). (a) The annual global sea-level change relative to the average over the period 1986-2005. All datasets are aligned to have the same value in 1993. (b) Global mean sea-level rise from 2006 to 2100 determined by multi-model simulations (21 models). All changes are relative to 1986-2005. Time series (lines) and projections of a measure of uncertainty (shading) are shown for the Representative Concentration Pathways (RCP) 2.6 (blue) and RCP 8.5 (red) scenarios.

The predominant effect of soil salinity is its effect on the soil water potential. As a result salinity strongly influences the water status of mangrove trees (Vandegehuchte et al., 2014b). Lambs & Saenger (2011), for example, found that the water uptake of *Ceriops tagal* showed an increase of about 39 % for species in near freshwater conditions (salinity of 3.5 ‰) compared to species in seawater (salinity of 35 ‰). These findings confirm the impact of salinity on water uptake and mangrove development. In this same research it appears that mangrove saplings are more affected by changes in salinity than by salinity itself. This is food for thought but remains out of the scope of this paper.

The most prominent factor discussed in the context of salinity is the rise in sea-level. Sea-level rise itself is a result of three predominant factors: (i) ocean thermal expansion, (ii) glacial melt and (iii) a change in terrestrial storage (Mitra, 2013). Nonetheless, the impact and significance of this sea-level rise is dependent on the salinity of seas and oceans surrounding the mangrove communities. It is generally assumed that a rise in sea level will push back mangrove zonation in an upstream direction. On the other hand, an increase in precipitation could also push back seawater for riverine mangroves by an increase in river

flow (Hogarth, 2007).
Inundation not only affects salinity but also reduces oxygen levels within the rooting zone. This can lead to the production of phytotoxins, a further reduction of water uptake (Vandegehuchte et al., 2014b) and a reduction in stomatal conductance (g_s) (Cardona-Olarte et al., 2013). Phytotoxins are by-products of soil reduction and can impose severe stress on plant roots (Pezeshki & De Laune, 2012).

Also anthropogenic withdrawal of groundwater has major effects on the availability and salinity of water for mangrove ecosystems. The impact of a sea-level rise due to climate change and the anthropogenic withdrawal of groundwater on mangrove ecosystems are illustrated in Figure 1.7. A significant negative correlation has been observed between salinity and chlorophyll content of mangrove leaves. This correlation significantly affects the rate of photosynthesis in this vegetation. The impact of salinity is not uniform for all mangrove species. It is sufficient to mention that an increase in salinity significantly ($p \leq 0.01$) decreases the concentration of chlorophyll in *A. marina* (Mitra, 2013).

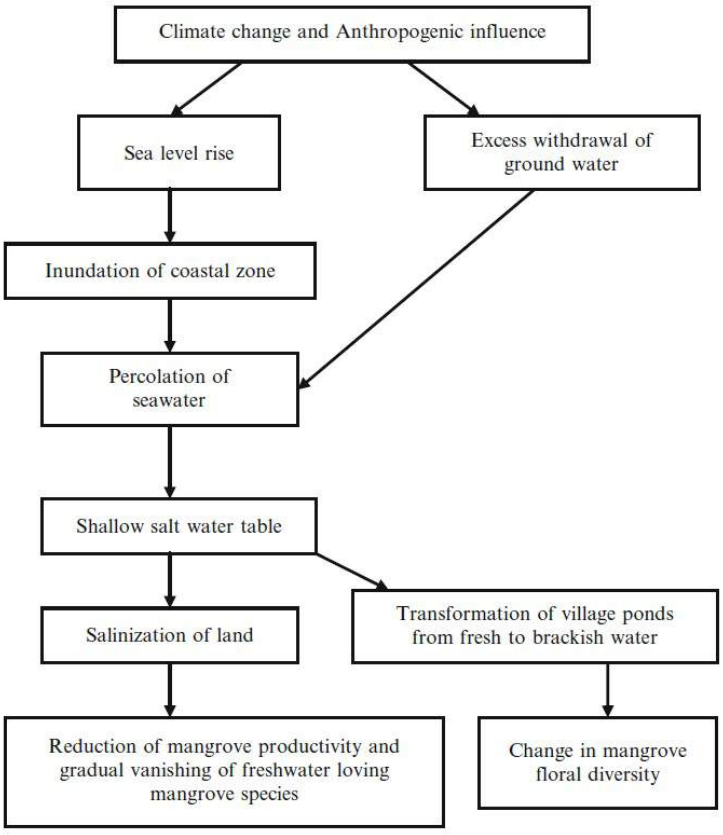

Figure 1.7: Impact of sea-level rise and anthropogenic withdrawal of groundwater on mangroves (Mitra, 2013).

1.4 Water in the soil-plant-atmosphere continuum

In the original SPAC hypothesis water moves unidirectional from soil, through plant to the atmosphere. Recent studies suggest however that this model might be incomplete and should be bi- or multidirectional. The most prominent suggested additions to this model are foliar water uptake (Goldsmith, 2013) and root pressure (Taiz & Zeiger, 2002; De Swaef et al., 2012). To come to the concept of foliar water uptake some other variables such as water potentials, the cohesion-tension theory, sap flow generalities, stem diameter variations and hydraulic redistribution should be discussed first.

1.4.1 Classical water transport

Taiz & Zeiger (2002) state the following (p. 40): *'Like the body temperature of humans, water potential is a good overall indicator of plant health.'*

This water potential is a measure of the free energy of water per unit of volume, and is a good indicator for the availability of water (Taiz & Zeiger, 2002). The numerical value is a relative value with a reference of 0 MPa for free water at 298 K under atmospheric pressure at sea-level (by definition) (Campbell et al., 2008; Lambers, 2008). Water movement follows the gradient from a higher to a lower, i.e. more negative, water potential (Taiz & Zeiger, 2002). In essence, this water potential gradient can be defined as the driving force for water transport between two locations in the SPAC (Steppe, 2004). The total water potential (Ψ) of plants consists of four components: the hydrostatic water potential (Ψ_p), the osmotic or solute potential ($\Psi_o = -R_g.T.C_o$; R_g $[J.mol^{-1}.K^{-1}]$: gas constant; T $[K]$: temperature; C_o $[mol.l^{-1}]$: osmolality), the gravity potential ($\Psi_g = \rho_w.g.h$; ρ_w $[kg.m^{-3}]$: density of water; g $[m.s^{-2}]$: gravitational acceleration; h $[m]$: height) and the matrix potential (Ψ_m) (Taiz & Zeiger, 2002; Steppe, 2004; Nobel, 2009).

However, the matrix potential can be neglected in wet soils which are predominant in mangroves and the gravitational component can be neglected near the surface (Ψ_g accounts for 0.01 $MPa.m^{-1}$) (Taiz & Zeiger, 2002). Even when soils in mangroves would dry the matrix potential can be represented by its contribution to the osmotic (thermodynamic activity) and pressure (capillary rise) potential (Nobel, 2009). By consequence the total water potential can be approximated by:

$$\Psi = \Psi_p + \Psi_o \tag{1.1}$$

Plants, such as mangroves, growing in a saline environment typically have very low values of Ψ_o in order to lower Ψ enough to extract water from salty water (Taiz & Zeiger, 2002). Scholander et al. (1964) reported xylem values of Ψ_p from -4.5 to -6 MPa for leaves of different mangrove species, measured with a pressure bomb. These values are similar to the range of -3.8 to -5.2 MPa reported by Lüttge (2008) and are far below the general applied permanent wilting point of -1.5 MPa for soils (Nobel, 2009). However, these values

are a necessity due to the low water potential (Ψ) of seawater of about -2.5 MPa (Tomlinson, 1986; Hogarth, 2007; Lüttge, 2008). As a consequence the low leaf water potential is a driver for the water uptake of mangroves (Suárez et al., 1998). However, salt-tolerant species, such as mangroves, have been known to have high amounts of mucilage in the xylem vessels. The low Ψ_p found with pressure bomb measurements in this case reflect the need to squeeze water out of the hydrogels rather then xylem pressures. The accumulation of mucilage in vessels and leaf plugs is an important water saving strategy and might be involved in moisture uptake from the atmosphere (Zimmerman et al., 2007).

Although the concept of water potentials explains the movement of water through plants, it does not explain where these hydrostatic pressure potentials in the xylem originate from. In order to explain this illusive concept the cohesion-tension theory was proposed by Henry Dixon and Charles Joly at the end of the nineteenth century (Nobel, 2009).

The cohesion-tension theory states that water evaporating from the leaf stomata develops a large tension (negative hydrostatic pressure) in the xylem originating from the cohesive properties of water, i.e. its hydrogen bonds, thus pulling the water column upwards through the SPAC by a passive process (Taiz & Zeiger, 2002; Nobel, 2009; De Swaef et al., 2012; Vandegehuchte et al., 2014b). Under these conditions the pressure potential in the plant is more negative than the vapor pressure of water, thus forcing the xylem sap in a metastable phase (Steppe, 2004). In the original theory water moves from soil, through the plant into the atmosphere, driven by a low water potential of the dry atmosphere and a relatively high water potential of leaves. The uptake of water through the roots is driven by the overall water potential gradient originating from transpiration (Goldsmith, 2013) which in turn is facilitated by solar energy used to overcome the latent heat of evaporating water (Steppe, 2004). As such, the drying force or evaporative demand of the atmosphere can be seen as the driving force behind sap flow in the SPAC (Nadezhdina et al., 2012).

Following the cohesion-tension theory, sap flow occurs passively in the xylem from root to leaf level. In case of a steady-state (water uptake by roots equals water loss by leaves) the van den Honert equation (Eq. 1.2) can be applied for sap flow (SF $[g.h^{-1}]$) in the SPAC. This equation states that SF equals the ratio of the difference in water potential ($\Delta\Psi$ $[mPa]$) over the hydraulic resistance (R $[MPa.h.g^{-1}]$) (Nobel, 2009). In other words, this equation states that the driving force of sap flow corresponds to a decrease in water potential (Steppe, 2004).

$$SF = \frac{\Delta\Psi}{R} \tag{1.2}$$

Yet, the condition of a steady-state is not always met. In order to meet this shortcoming the van den Honert equation has been expanded with hydraulic capacities (C) defined as the ratio of the difference in water content (dW) over the difference in water potential ($d\Psi$) (Figure 1.8) (Steppe, 2004; Nobel, 2009).

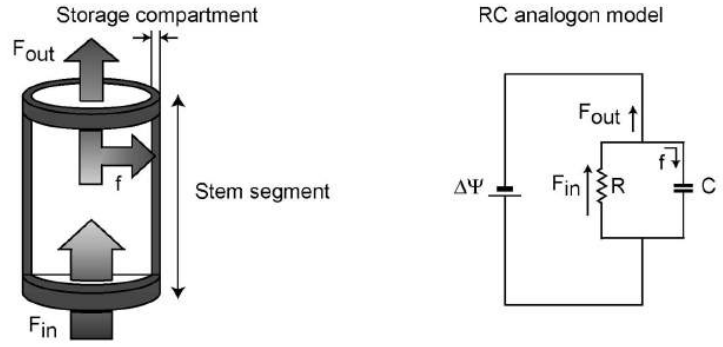

Figure 1.8: Left: Schematic view of dynamic water flow through a stem segment. Right: Electrical RC analogon model for dynamic water flow (Steppe, 2004).

Assuming that the difference in water content equals sap flow minus transpiration (E $[g.h^{-1}]$) (Eq. 1.3), while $\Delta\Psi$ can be stated as the difference between Ψ_{soil} and Ψ_{leaf}, differential equation 1.4 can be derived when applying equation 1.3 and the hydraulic capacities to the leaf level (Nobel, 2009).

$$f = \frac{dW}{dt} = F_{in} - F_{out} = SF - E \tag{1.3}$$

$$\frac{d\Psi_{leaf}}{dt} + \frac{\Psi_{leaf}}{R.C} = \frac{\Psi_{soil} - E.R}{R.C} \tag{1.4}$$

It has been shown that a time lag exists between E and SF. As a result of this lag between water uptake and water loss stem diameter variations (SDV) occur (Steppe, 2004; Steppe et al., 2015a). However, SDV are a result of multiple processes. Most predominant processes are linked to reversible shrinkage and swelling due to the hydration state of tissue (Vandegehuchte et al., 2014a). When transpiration starts in the early morning, first the internal reserves originating from water storage capacities are depleted in order to meet the high water demand at leaf level. This depletion occurs due to a lowered leaf water potential (Nobel, 2009; De Groote et al., 2013; Vandegehuchte et al., 2014b) which results in a decrease in xylem water potential. As a consequence the xylem water potential is lower than the storage water potential resulting in a water flow from storage tissue to the xylem conduits by a pathway of radial diffusion (Vandegehuchte et al., 2014a). When the trunk has a higher capacitance, the lag between water demand and water supply at the root level increases. This radial flow causes a shrinkage of the stem diameter (Steppe et al., 2006; Vandegehuchte et al., 2014a). Embolisms also release water into the xylem conduits,

thus smoothing large changes in xylem tension (Steppe et al., 2015a). When transpiration diminishes later that day, water potential in the xylem rises above the water potential in the storage tissue allowing a positive sap flow from the soil to the trunk (Steppe et al., 2006; Vandegehuchte et al., 2014a), thus replenishing the internal reserves and causing an increase in diameter (Steppe et al., 2006; Nobel, 2009; De Groote et al., 2013; Vandegehuchte et al., 2014a,b) (order of magnitude 0.3 to 1 % of the total diameter) (Nobel, 2009).

Furthermore, mangrove species have been known to synthesize and accumulate organic (e.g. proline, mannitol and cyclitol) and inorganic (e.g. sodium and potassium) substances respectively, in their leaves in order to decrease Ψ_o (Reef & Lovelock, 2014; Vandegehuchte et al., 2014b,a). It is likely that these processes also occur at stem level, lowering the water potential and thus influencing within-day SDV patterns (Vandegehuchte et al., 2014b,a) by varying Ψ_o of the storage tissue (Figure 1.9) (Vandegehuchte et al., 2014a).

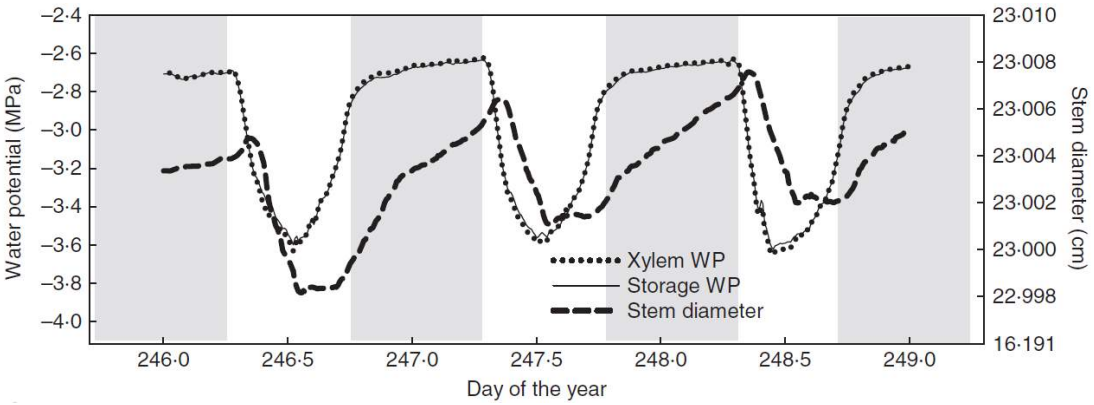

Figure 1.9: Model results with stem diameter input and xylem and storage water potential (WP) output for *Avicennia marina* (Vandegehuchte et al., 2014a).

1.4.2 Growth

In addition to reversible SDV, irreversible growth takes place. The predominant model used to assess enlargement of cells during growth is the model of Lockhart (1965) (Eq. 1.5). This equation expresses that growth rate (i.e. the relative volume change, $\frac{dV}{V.dt}$) is driven by a positive Ψ_p, i.e. turgor, when a critical threshold value Γ [MPa] is exceeded. The proportionality factor between growth and this driving factor is defined as the cell wall extensibility (ϕ $[MPa^{-1}.s^{-1}]$) (Steppe, 2004). When water flow occurs into a cell, the cell volume will irreversibly change if cell wall extension takes place (Steppe et al., 2006), i.e. the difference between Ψ_p and Γ determines irreversible growth (Steppe et al., 2015a).

$$\frac{dV}{V.dt} = \phi(\Psi_p - \Gamma) \tag{1.5}$$

At night, when water uptake continues, the internal water reserves are replenished and

the hydrostatic water potential increases which facilitates growth (Hubeau et al., 2014). If Γ is not exceeded, for example in a state of stress during the dry season, a decreasing diameter trend may occur indicating an unfavorable water and/or carbon balance and a state of stress. Small daily variations in salinity have little effect on SDV. However, high salinity is likely to restrict water uptake and possibly causes a decrease in stem diameter (Vandegehuchte et al., 2014b).

In general *A. marina* prefers freshwater areas. However, in natural conditions they are out-competed by other vegetation in these areas. When freshwater like freshwater lenses or water with a reduced salinity due to rainfall is available, they are more likely to use this less saline water (Lambs & Saenger, 2011). Periods of high stem swelling have been observed for mangroves species in periods of rainfall (Hubeau et al., 2014). In this respect it appears plausible that mangrove species use FWU (section 1.4.4) as a source of freshwater in order to meet the required turgor for growth. Nevertheless, Suárez et al. (1998) suggested that as a result of adaptations such as an increased solute concentration and cell elasticity of leaves, species grown in a high salinity environment could hold leaf turgor over a larger range of Ψ_{soil}.

It has been suggested that growth of *A. marina* is larger during rainy seasons due to a decrease in salinity. However, other factors concomitant with precipitation might also be of importance such as a change in tidal level, temperature and nutrient availability (Nazim et al., 2013) as well as the possibility of FWU. Schmitz et al. (2008) stated that optimal growing conditions could stimulate the differentiation of new cambium, resulting in multiple simultaneous growth layers with their own xylem and phloem bands (Figure 1.10). However, also a patchy growth of successive cambia has been indicated for *A. marina*, implying that not the entire circumference increases simultaneously. Patchiness is, however, a potential adaptation rather than a systematically present feature. By assessing a patchy growth *A. marina* can focus water supply without dehydrating during severe physiological drought. The patches are spatio temporal variable, as such over a longer time period the whole trunk gets hydrated. Patchiness is independent of leaf and branch formation (Robert et al., 2014).

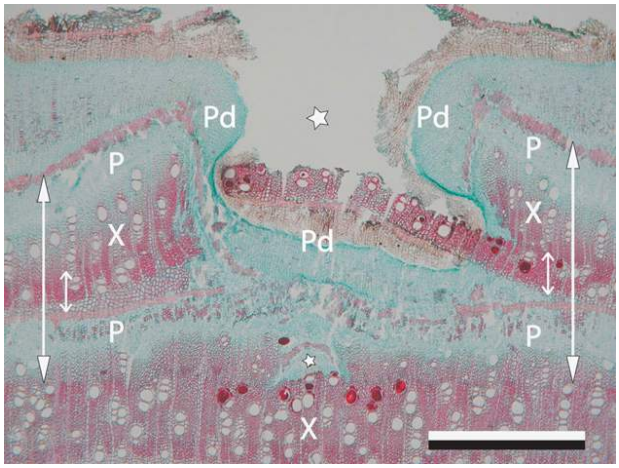

Figure 1.10: Transverse microsections of the stem wood of *A. marina* after wounding of the two outermost cambia. Scale bar = 1 mm. P: Phloem band; Pd: Periderm; X: Xylem band; Large arrows: Radial increment from February 2006 to June 2006; Small arrows: Part of the growth layer already formed at the time of cambial marking; Asterisks: Pinhole (Schmitz et al., 2008).

1.4.3 Hydraulic redistribution

When transpiration is absent, water moves passively through the SPAC towards the lowest Ψ. This redistribution of water is a consequence of competing Ψ, called hydraulic redistribution (HR) (Nadezhdina et al., 2009, 2010). There are several types of HR. Figure 1.11 illustrates the three known types: vertical HR (VHR, subdivided in hydraulic lift (HL) and hydraulic descent (HD)) horizontal HR (HHR) and tissue dehydration (TD) (Nadezhdina et al., 2010). While it has been suggested that night transpiration due to a nonzero vapor pressure deficit (VPD [kPa]) could limit HR, Nadezhdina et al. (2009) demonstrated that a significant HR is still possible under these conditions.

When discussing HR, Ψ is of primary importance. This water potential determines the direction of water movement through the SPAC. When tissue or soil dries out, Ψ of this element will decrease resulting in a passive flow towards the soil or tissue when transpiration has stopped. In case of mangroves, however, soil Ψ_o is low due to the high salinity. The considerable negative Ψ tends to extract water from mangrove-roots which has a large impact on HR in mangrove species (Lambs & Saenger, 2011). Furthermore, it should be noted that soil salinity can vary spatially due to local salt accumulations.

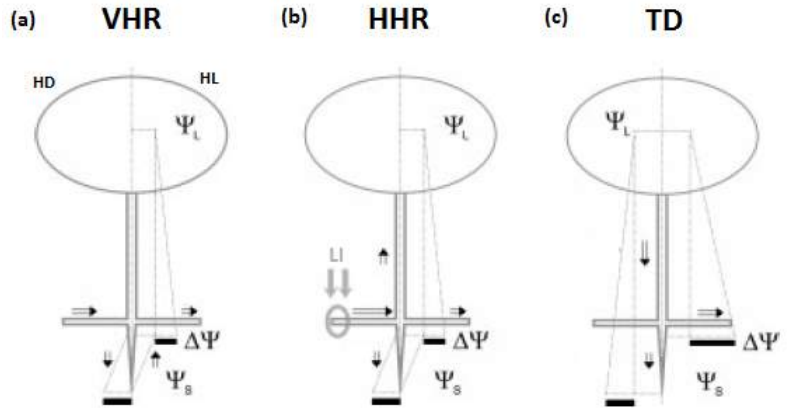

Figure 1.11: Three potential scenarios for hydraulic redistribution based on gradients in water potential (Ψ [MPa]); Ψ_L: leaf water potential; Ψ_s: soil water potential; $\Delta\Psi$: difference between Ψ_L and Ψ_s. Arrows indicate water flow (Nadezhdina et al., 2010). (a) Vertical hydraulic redistribution (VHR) subdivided in hydraulic lift (HL) and hydraulic descent (HD). (b) Horizontal hydraulic redistribution (HHR) as a consequence of localized irrigation (LI). (c) Tissue dehydration (TD).

As a result of VHR, water from deep soil layers can be transported upwards to the top soil. This is called HL (Nadezhdina et al., 2009, 2010). Water transported to these higher soil layers can be used by the tree itself the subsequent day, or by the surrounding vegetation. By VHR also groundwater reservoirs can be replenished. This is called HD or reverse HL (Nadezhdina et al., 2010). Both of these VHR can occur in mangrove ecosystems, stimulated by a salt gradient. Salt will accumulate in the topsoil due to inundation leading to HL at night. On the other hand, when rain occurs, the topsoil gets diluted resulting in HD.

When rain is direction-specific, or when a root reaches a freshwater-pocket, one root can have plenty of water while another root of the same tree can be near dehydration. In this case water flow will be dominated by the watered root during transpiration. When transpiration stops, however, water can flow from the wet root to the dry root. This HR is called HHR. Even though there is a difference in the proportion of water used by both roots, this redistribution has no effect on the total average water uptake of the tree. During daytime the uptake of wet roots will increase, while the uptake of dry roots decreases. At night HHR takes place, partially replenishing the dry soil around the dry roots. As a result no increase in total tree transpiration takes place (Nadezhdina et al., 2009, 2010).

TD only occurs in extreme conditions of prolonged drought or frost. Both cases are driven by a drop in Ψ_{soil} resulting in a significant water potential gradient between soil and leaves. This consequently leads to a reverse sap flow. The only source of water used in this type of HR is stored tissue water. This water storage should be replenished in order for the plant to survive in the long term. TD may be a crucial survival strategy for some species, as TD can be used to protect the roots by preventing dehydration (Nadezhdina et al., 2010).

In practice hydraulic redistribution can be assessed through stable isotope tracing. Isotopes most frequently used are ^{2}H and ^{18}O. However, this application relies on the assumption that no fractionation occurs during the uptake of water. This is not the case for all plants, as Ellsworth & Williams (2007) stated that uptake of water by the roots of xerophytes leads to a fractionation resulting in a decrease of ^{2}H in the roots compared to the surrounding soil. They also found a significant positive correlation between fractionation and salinity tolerance of xerophytes. This might also be of primary importance for *A. marina* when applying this method. It is hypothesized that fractionation occurs as water moves symplastically through cell membranes. This should be taken into account when assessing FWU as it is not known whether FWU occurs symplastically or apoplastically.

1.4.4 Foliar water uptake

In case of foliar water uptake (FWU) water moves from the atmosphere, forms a thin water layer on the leaves and goes to or through the plant into the soil, i.e. a complete reversal of the traditional SPAC-flow (Goldsmith, 2013). This phenomenon is of exceptional importance when air humidity reaches 100 %, e.g. under foggy conditions, dew or drizzle (Nadezhdina et al., 2010; Eller et al., 2013). Due to this high humidity VPD drops and the leaf water potential is close to zero, resulting in the uptake of water and flow to tissues or soil with a lower Ψ (Nadezhdina et al., 2010). In essence HR occurs (Goldsmith, 2013; Oliveira et al., 2014). Despite the low sap velocities of 1-1.5 $cm.h^{-1}$ approaching the limits of accurate sap measurements (Burgess & Dawson, 2004), this phenomenon can be of primary importance in the need of water for refilling tissue water reserves (Nadezhdina et al., 2010) and embolisms repair (Burgess & Dawson, 2004; Oliveira et al., 2014). However, it has been suggested that vessels can only be repaired a limited number of times. This is known as cavitation fatigue. This phenomenon has not been studied in mangroves, so the extend of this feature for *A. marina* is not known (Reef & Lovelock, 2014). Eller et al. (2013) observed an enhancement of leaf water potential, photosynthesis, stomatal conductance and plant growth due to FWU of fog water that was transported through the xylem. The driving force for FWU is a $\Delta\Psi$ between source and sink, in this case respectively air and leaves. The order of magnitude of FWU also depends on the FWU efficiency from source to sink ($k_{source-sink}$ $[m.s^{-1}.MPa^{-1}]$) (equation 1.6) (Oliveira et al., 2014).

$$FWU = k_{source-sink}.\Delta\Psi_{source-sink} \tag{1.6}$$

FWU has been proven for several species, for example in tropical montane forests (Goldsmith et al., 2013) or coastal redwood forests (Burgess & Dawson, 2004). In total at least 70 species have been proven to be capable of FWU, which represents over 85 % of all studied species suggesting that FWU is a widespread phenomenon. This property is tightly coupled to leaf wetting events. However, there is a large difference in FWU quantities among different species. This means that if climate change affects precipitation patterns,

not all species will be affected in a similar way (Goldsmith et al., 2013). Nonetheless, the pathways concomitant with the FWU scenarios (Figure 1.12) are poorly understood (Burgess & Dawson, 2004).

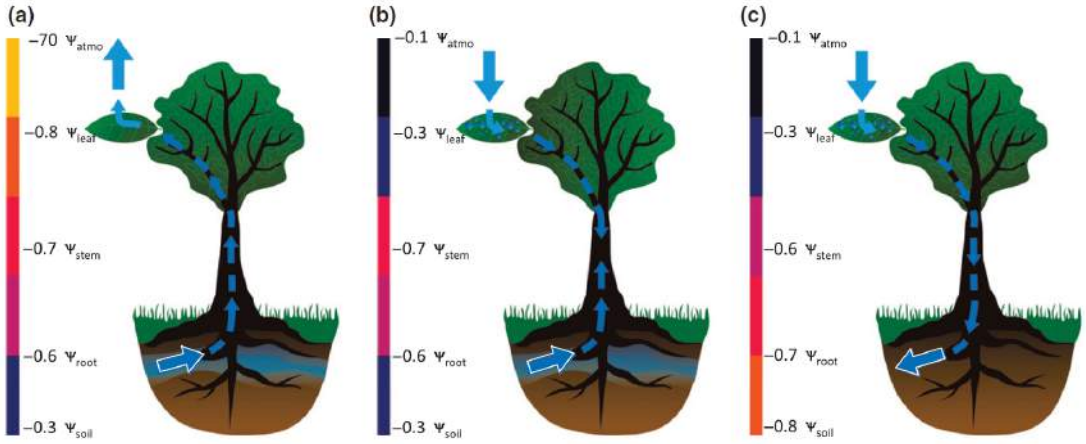

Figure 1.12: Three potential scenarios for the movement of water through plants based on gradients in water potential (Ψ [MPa]), illustrated by indicative values (Goldsmith, 2013). (a) Water movement caused by transpiration, i.e. a normal soil-plant-atmosphere (SPAC) flow. (b) Water movement caused by foliar water uptake during a leaf wetting event whilst simultaneously moving from a higher Ψ_{soil} to a lower Ψ_{stem}. (c) Water movement caused by foliar water uptake during a leaf wetting event resulting in water flow from leaf to soil, i.e. a complete reversal of the SPAC flow.

While it has been proven that Ψ has improved due to FWU, research has indicated that the difference in water potential might not fully correspond with the magnitude of FWU (Goldsmith et al., 2013; Goldsmith, 2013). Even more, only when water is formed on the leaf surface by condensation or when it comes into contact with the leaf surface through fog and the leaf is experiencing a water deficit, it is probable that the leaf tissue has a lower water potential then the boundary layer. As such, FWU is most likely when soil water availability is limited (Goldsmith, 2013). However, it has been stated by Burgess & Dawson (2004) that high water stress reduces FWU for *Sequoia sempervirens*. This decrease in FWU might be caused by a restriction in the water-uptake pathway rather than by changing water potentials, thus reducing hydraulic conductivity. The conductivity might be aided by specific leaf traits such as trichomes (epidermical outgrowths), hydathodes (Goldsmith et al., 2013; Goldsmith, 2013) cuticle permeability (Eller et al., 2013; Oliveira et al., 2014) and leaf plugs filled with mucilage (Zimmerman et al., 2007). It is assumed that the ability of some species to exudate water through hydathodes is correlated with their ability to absorb water through FWU. As cuticular transpiration is a known process (Steppe, 2004; De Groote et al., 2013), a type of reverse cuticular transpiration or cuticular

uptake could be one of the possibilities, for example in the absence of hydathodes. It has been stated that old leaves are better suited for FWU presumably due to the occurrence of features such as cracks in the cuticle and general decay of the leaf surfaces or fungal hyphae conducting water and entering the stomata. It should be stated, however, that cuticle wettability and permeability vary considerably among species (Burgess & Dawson, 2004). It can be concluded that the control of FWU is species and environmental dependent.

The advantages of FWU for *A. marina* lie in the enlarged water availability like for any other species. However, due to the fact that *A. marina* grows in brackish and salty water this species is almost under a constant state of physiological drought increasing the importance of a fresh water source.

Uddin et al. (2014) found a downward sap flow dynamic concomitant with an increase in stem diameter when applying an artificial rain event on *A. marina* (Figure 1.13). These findings imply foliar uptake of water by *A. marina*, as in these tests the petioles and stem were covered to prevent direct contact with water. However, these tests took place on an insufficient number of trees without repetition nor adequate control group. Therefore these results are promising but inconclusive.

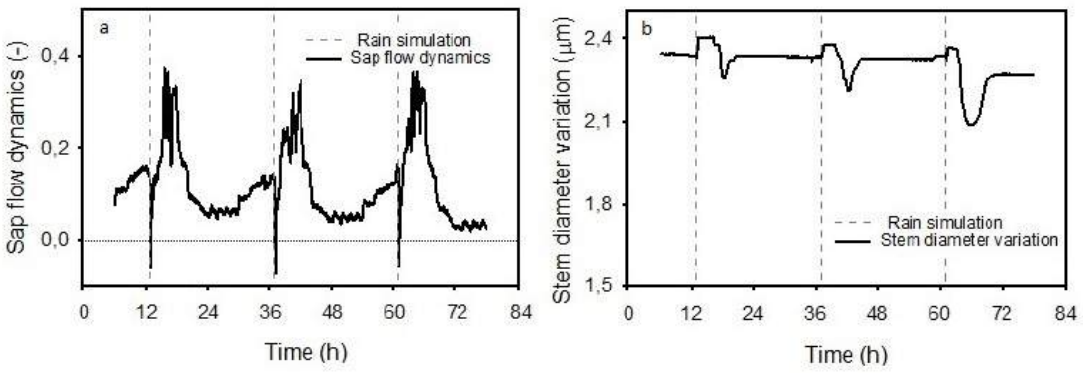

Figure 1.13: (a) Sap flow dynamics and (b) stem diameter variations of *A. marina* during artificial rain simulations. The horizontal dotted line indicates the zero line. The vertical dashed lines represent time of rain simulation (Uddin et al., 2014).

Chapter 2

Materials and methods

2.1 Experimental set-up

In order to germinate and grow *A. marina* a controlled experimental set-up was constructed. The experiments took place in a greenhouse (2 x 2.5 x 4 m) at the Laboratory of Plant Ecology, University Ghent (51°3′13" N, 3°42′31" E).

A. marina propagules originating from Australia (−33°50′40" S, 151°4′50" E) were planted in pots halfway into the substrate (Appendix A) on the 19th of January 2015. In addition seedlings were planted. Propagules and seedlings together resulted in 22 surviving plants out of 32. The substrate used was a self-made mixture of approximately 15 % peat, 15 % mangrove mud and 70 % river sand. Pots with a height of 12 cm and a diameter of 16 cm were placed in gutters of 1.80 x 0.25 x 0.12 m, with a density of 7-8 pots per gutter. In order to simulate semi-natural conditions, tides were simulated in the gutters with a pump-valve-system and barrels of 30 liter. Twice a day there was high and low tide (Figure 2.1), however, tidal progression was not taken into account. Tide started at 7 am resulting in high tide at 8 am. This was maintained for 5 hours. Starting from 1 pm water level started to decrease until 2 pm. Low tide was maintained for 5 hours. At 7 pm the cycle restarted. Tidal water was tap water with an addition of 20 g sea-salt per liter of water, resulting in a salinity of 19.6 ‰ or a theoretical Ψ of -1.45 to -1.65 MPa depending on the temperature (approximately 10-40 °C respectively).

Fertilization took place with 0.84 gram of N:P:K 20:20:20 per liter on the 9th of March in order to stimulate growth, in accordance with López-Hoffman et al. (2007).

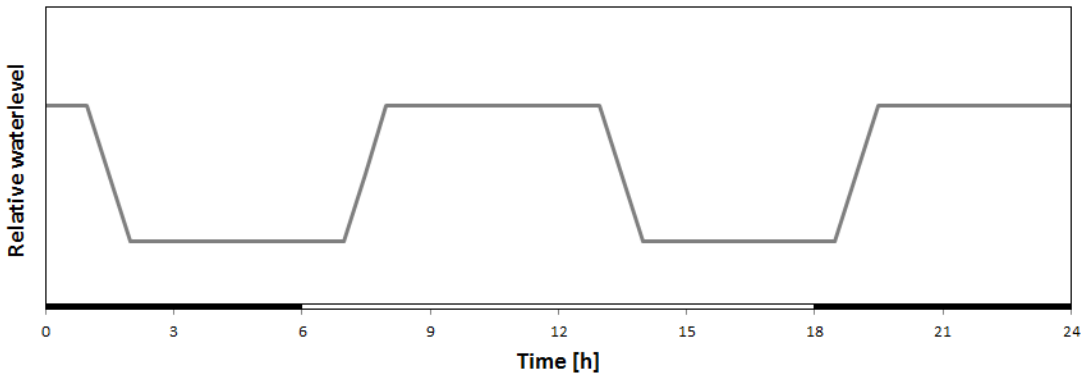

Figure 2.1: Relative tides during the time span of one day. White and black bars at the bottom indicate respectively when artificial lights are on and off.

2.1.1 Biotic parameters

A. marina seeds are highly sensitive to dehydration and cooling. As a result, they were kept moist and warm during the whole germination period. The different development stages of an *Avicennia* seedling are shown in Figure 2.2. Germination, however, only occurs when the pericarp has been shed or removed due to inhibition originating from a high level of abscisic acid (ABA) present in the pericarp (Farrant et al., 1993a) and an increased chance of coverage with microbial contamination when the pericarp is not shed (Farrant et al., 1993b). Shedding naturally occurs as a consequence of swelling when coming into contact with tidal water (Farrant et al., 1993a). Sensitivity to dehydration increases as germination progresses (Farrant et al., 1993b). In order to avoid dehydration, propagules and seedlings were sprayed regularly with tap water.

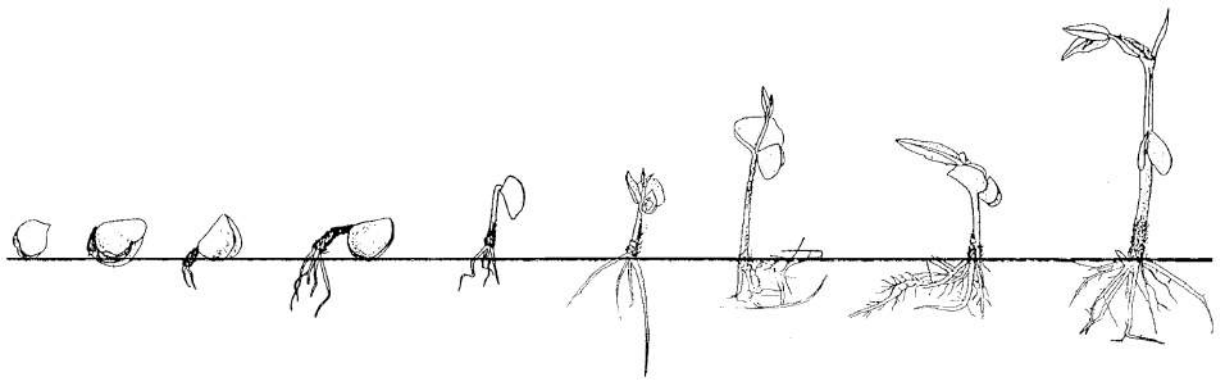

Figure 2.2: The development of an *Avicennia* seedling (Hogarth, 2007)

2.1.2 Abiotic parameters

During germination and growth relative humidity (RH [%]) and temperature (T [$°C$]) are of primary importance. In order to keep the RH sufficiently high two humidifiers (Ultrasonic U7135, Boneco, Widnau, Switzerland) were used (Figure 2.3). In order to measure the reached RH and T a humidity and temperature sensor (SHT 25, Sensirion, Staefa, Switzerland) was used.

Figure 2.3: Humidifier (Ultrasonic U7135, Boneco, Widnau, Switzerland)

Vapor Pressure Deficit (VPD [kPa]) is a function of RH and air temperature (T_{air} [$°C$]). This variable indicates the drying power of the surrounding air and is defined as the difference between the saturation vapor pressure (e_o^v [kPa]) and the actual vapor pressure (e^v [kPa]) (equation 2.1) (Abtew & Melesse, 2013; De Groote et al., 2013).

$$VPD = e_o^v - e^v \tag{2.1}$$

e_o^v and e^v can be calculated by equation 2.2 and 2.3 respectively (Abtew & Melesse, 2013; De Groote et al., 2013).

$$e_o^v = 0,611.exp\left(\frac{17,27.T_{air}}{T_{air} + 237,3}\right) \tag{2.2}$$

$$e^v = e_o^v.\frac{RH}{100} \tag{2.3}$$

In order to create more photosynthetically active radiation (PAR) two lamps (Master HPI-T Plus lights 400 W, Philips, Eindhoven, Netherlands) were used in addition to natural sunlight. The emitted spectrum of these lamps is illustrated in Figure 2.4. Assimilation lamps were turned on and off at 6 am and 6 pm respectively. PAR was measured with a sun calibration quantum sensor (SQ-110, Apogee, Logan, United States of America).

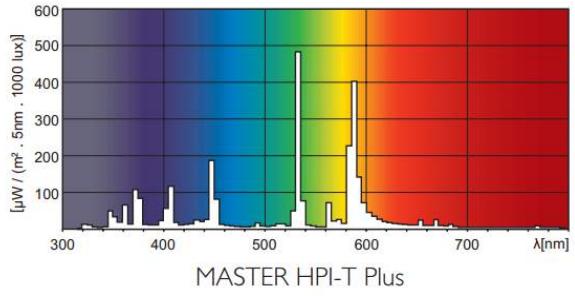

Figure 2.4: Emitted spectrum of lamps (Master HPI-T Plus lights 400 W, Philips, Eindhoven, Netherlands) (Philips, 2014)

2.1.3 Treatments

Simulation of artificial rain events were performed by spraying tap water onto the leaves during different time periods. Prior to the start of the different treatments the petioles, stems and soil were covered with aluminum foil and tape to prevent an additional uptake of water by other plant organs (subsection 2.2.2). The effects of rain simulation were observed with sapflow sensors (mini HFD, University Ghent, Ghent, Belgium; section 2.2.1) and linear variable displacement transducer (LVDT; DF 5.0, Solartron Metrology, Bognor Regis, United Kingdom; section 2.3) sensors.

The first sap flow experiment consisted of 2 artificial rain events of 1 hour on day of the year (DOY) 92 and 93 from 9.30 - 10.30 am. The second sap flow experiment consisted of 2 artificial rain events of 2 hours on DOY 96 and 97 from 9.30 - 11.30 am. The first water potential experiment consisted of 1 artificial rain event on DOY 98 from 10.20 - 11.50 am. The second water potential experiment consisted of 1 artificial rain event on DOY 113 from 9.30 am - 1.00 pm. The deuterium control experiment consisted of 1 artificial rain event on DOY 124 from 9.30-10.30 am with tap water. The deuterium experiment consisted of 1 artificial rain event with deuterated water on DOY 125 from 9.40-10.40 am.

2.1.4 Logging

All T-, RH-, PAR- and LVDT-data were recorded with a datalogger constructed at the Laboratory of Plant Ecology, Ghent University, and the Phytosense software of Phyto-IT.

All HFD-data were recorded at 10 second intervals and averaged every 60 seconds with a Campbell datalogger (CR1000, Campbell Scientific Inc.,Logan, United States of America).

2.2 Sap flow

2.2.1 Heat field deformation method

Recently a non-invasive sap flow sensor based on the heat field deformation (HFD) method has been constructed by Hanssens et al. (2013). This so called mini HFD (Figure 2.5) is ideal for measuring sap flows in saplings due to its small size and light weight. These mini HFD-sensors were reconstructed by sewing an SMD (Surface-Mounted Device) of 100 Ω and three Copper-Constantan thermocouples (type T) on a piece of foam insulation tape (Armaflex) with nylon thread. A continuous voltage of 3 V was applied to the SMD. The tape is stuck to the stem of the plant just below the lowest leaves. Subsequently the sensor is wrapped with bubble wrap for insulation purposes and finally with aluminum foil to reflect incident radiation.

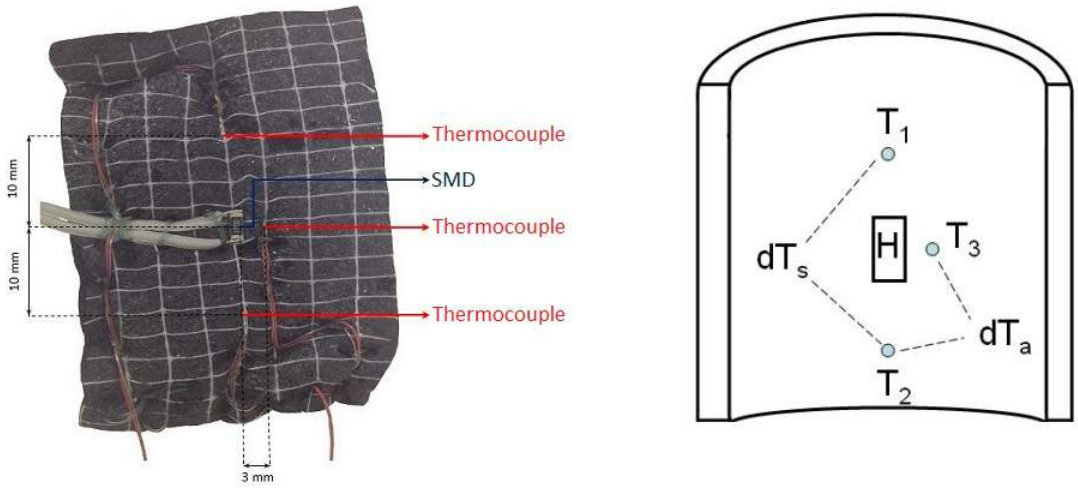

Figure 2.5: Left: Build-up of a mini HFD sensor: Copper-Constantan Thermocouple; SMD = Surface-Mounted Device of 100 Ω. Right: Schematic build-up of a mini HFD sensor (Hanssens et al., 2013).

When assessing SF, first the temperature difference between the upper and lower thermocouple (dT_{sym}) is calculated. This difference allows for both bi-directional and low sap flow measurements. Secondly the temperature difference between the lower and tangential thermocouple (dT_{as}) is calculated in order to be able to distinguish high from low SF. The ratio of dT_{sym}/dT_{as} follows a linear relationship with the temperature difference between the upper and tangential thermocouple (dT_{s-a}). When extrapolating this linear relationship, the vertical displacement relative to the x-axis ($dT0_{s-a}$ or K-value: the absolute value of this displacement or sensu stricto the dT_{s-a} value for zero flow) can be defined (Nadezhdina et al., 2012; Vandegehuchte & Steppe, 2012; Forster, 2014). In general, this K-value can be determined by either extrapolating dT_{s-a} or dT_{as}. Due to a better linear relationship dT_{s-a} (Figure 2.6) will be used in this paper. By consequence, the need of

an actual zero flow, which is difficult to encounter, is eliminated (Nadezhdina et al., 2012; Vandegehuchte & Steppe, 2013).

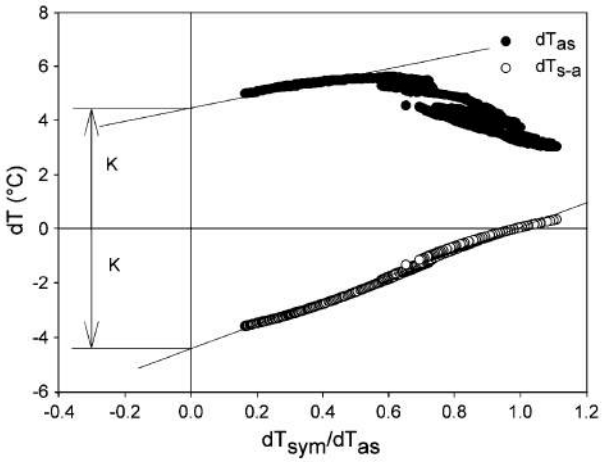

Figure 2.6: Temperature differences dT_{as} and dT_{s-a} with an illustration of the resulting K-value (Nadezhdina et al., 2012)

In order to calculate SFD with the classical HFD-sensor some factors need to be known and quantified: the thermal diffusivity (D $[cm^2.s^{-1}]$), the axial distance between the upper/lower needle and the heater (Z_{ax}), the distance between the tangential needle and the heater (Z_{tg}) and the measuring depth into the sapwood at the location of the sensor (L_{sw}) (Vandegehuchte & Steppe, 2012; Forster, 2014). Subsequently the SFD can be calculated as:

$$SFD = 3600.D.\frac{Z_{ax}}{Z_{tg}}.\frac{1}{L_{sw}}.RSF \tag{2.4}$$

The HFD-ratio (RSF) represents the dynamic part of the SFD equation (Hanssens et al., 2013) and is calculated as follows:

$$RSF = \frac{dT0_{s-a} + dT_{s-a}}{dT_{as}} \tag{2.5}$$

It has been experimentally proven that RSF is highly correlated with the SFD (Vandegehuchte & Steppe, 2012). However, measured SFD are strongly dependent on the thermocouple positioning (Hanssens et al., 2013). SF can be calculated as the product of the SFD and the cross sectional area.

In order to measure the actual SF with the mini HFD sensor, a destructive calibration is needed after measurement. Due to time limitations only relative sap flow dynamics were measured by calculating RSF. Actual SF was not taken into account. However, when starting the calibration it has been found in this study that a better calibration can be

found when the K-value is discarded (Appendix B).

As such the HFD-ratio can be simplified to:

$$RSF_s = \frac{dT_{s-a}}{dT_{as}} \tag{2.6}$$

The resulting calibration between SF and RSF_s has a better fit (R^2), e.g. in extremis 0.94 compared to 0.48.

2.2.2 Considerations

When trying to assess FWU caution should be taken regarding the used measuring technique. Fully submerged leaves for example might establish different conditions for FWU than leaves in a natural state. Water will first be used to replenish dehydrated upper parts of the species, possibly before reaching a sap flow sensor. In addition, the age and water status of a specific leaf will influence measured result. As such, measurements from one type of leaf cannot be up-scaled to a whole canopy (Burgess & Dawson, 2004).

To ensure that the measured relative SF resulted from FWU, first the potential stem water uptake (SWU) was assessed by inducing an artificial rain event on plants with covered leaves and roots (Figure 2.7). As SWU took place (data not shown), stems were covered during the sap flow experiments in order to assess FWU.

Figure 2.7: Left: Assessing stem water uptake (SWU) by an artificial rain event on plants with covered leaves and soil. Right: Plants with covered stems in order to assess foliar water uptake (FWU) without SWU. Roots were only covered during artificial rain events in order to avoid additional anoxic conditions. Part where linear variable displacement transducer (LVDT) sensor touched the plant was not covered during the experiment.

2.3 Stem diameter variation

Stem diameter variations were measured in order to make a distinction between reversible SDV and irreversible growth. The LVDT sensor used (DF 5.0, Solartron, Bognor Regis, United Kingdom; Figure 2.8) has a measurement range of 10 mm (Solartron, 2015). When the diameter increases a small metal rod with a return spring is pushed inward resulting in a higher mV output. Sensors were installed as illustrated in Figure 2.7.

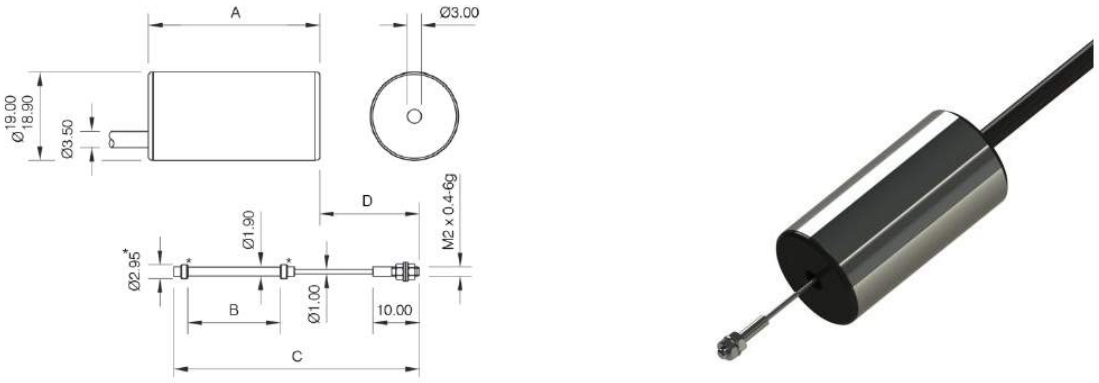

Type	A	B	C	D
DF5 / DFg5	43.0	24.3	57.3	20.5

Figure 2.8: Solartron DF 5.0 specifications, dimensions in mm (Solartron, 2015)

2.4 Water potential

Water potentials were measured with a thermocouple-psychrometer (HR-33T, ELITech-Group Wescor, Logan, United States of America; Figure 2.9) by usage of three sample chambers (C-52, ELITechGroup Wescor, Logan, United States of America; Figure 2.10). Samples were taken with a paper punch. First samples were taken at the tip of the leave, gradually descending to the base in a zigzag way in order to reduce influence of previous samples on the current sample. Irrigation water was sampled by submerging paper punched circles of filtration paper into the irrigation water. Measurements of the irrigation water took place after the first artificial rain event, hence a dilution might have already taken place. All measurements were recorded with a two channel strip chart recorder (PM8262, Philips, Eindhoven, Netherlands; recorder on Figure 2.9 and output on Figure 2.11).

The output of the strip chart recorder was analyzed manually at a preset time of 5 seconds following the start of evaporation. The measured voltage was converted to its respective water potential through calibration of each individual sample chamber.

Figure 2.9: The thermocouple-psychrometer (HR-33T, ELITechGroup Wescor, Logan, United States of America) on the left and the strip chart recorder (PM8262, Philips, Eindhoven, Netherlands) on the right.

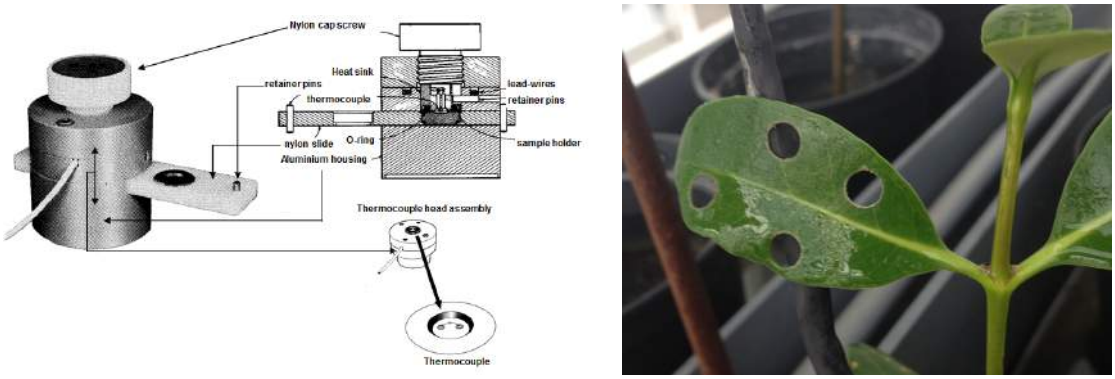

Figure 2.10: Left: Sample chamber (C-52, ELITechGroup Wescor, Logan, United States of America) of the thermocouple psychrometer (HR-33T, ELITechGroup Wescor, Logan, United States of America). Right: Leaf with cut out samples by paper punch.

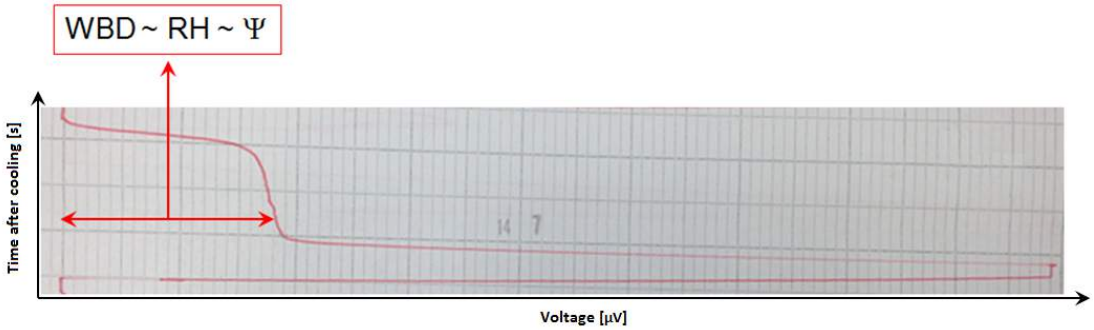

Figure 2.11: Output of the channel strip recorder (PM8262, Philips, Eindhoven, Netherlands). WBD = Wet bulb depression; RH = Relative humidity; Ψ = Water potential.

2.5 Foliar uptake capacity experiment

To ensure uptake of water through leaves took place, a foliar water uptake experiment was performed, adapted from Burns et al. (2009). In this experiment 10 leaves were cut at the petiole as close as possible to the stem and divided in 4 old (lower leaves, approximately 3-4 months old) and 6 young (middle and upper leaves, approximately a few weeks to 2 months old) leaves. Most of the older leaves showed some small necroses.

Leaves were patted dry and salt from the leaf surface was carefully removed with paper towel. Subsequently leaves were weighted and taped to petri dishes with petioles as high as possible. Petioles were closed off with tape in order to avoid transpiration. Petri dishes were filled with distilled water until leaves were submerged. Due to the small size of the petioles the leaves were not fully submerged in order to avoid contact of the petioles with water. Petri dishes were placed in the dark in order to avoid transpiration by not submerged parts. After 3 hours leaves were patted dry and weighted. Subsequently leaf area was measured resulting in an estimation (leaves not totally submerged) of water uptake per unit of leaf area ($Uptake.Area^{-1}$ $[g.cm^{-2}]$). Water $Uptake.Area^{-1}$ was calculated as:

$$Uptake.Area^{-1} = \frac{Mass_2 - Mass_1}{Area} \tag{2.7}$$

With $Mass_1$ $[g]$ the leaf mass before submergence, $Mass_2$ $[g]$ the leaf mass after submergence and Area the total leaf area $[cm^2]$. Last, leaves were dried at $70 - 90$ $°C$ until leaves were oven dry after which leaves were weighted ($Mass_{dry}$). Difference in leaf water content (ΔLWC [%]) was calculated for leaves before and after the submergence treatment as:

$$\begin{aligned}\Delta LWC &= \frac{Mass_2 - Mass_{dry}}{Mass_2}.100 - \frac{Mass_1 - Mass_{dry}}{Mass_1}.100 \\ &= \frac{Mass_{dry}(Mass_2 - Mass_1)}{Mass_1.Mass_2}.100\end{aligned} \tag{2.8}$$

2.6 Hydraulic redistribution

Hydraulic redistribution can be assessed through isotope tracing with deuterium, a stable hydrogen isotope (^2H or D). By actively accumulating this isotope heavy water can be created with a high concentration of deuterium oxide (D_2O). Nonetheless, deuterium tracing is not recommended when estimating total plant water use due to a possible overestimation. This method is suitable for estimating HR and water storage processes within plants (Schwendenmann et al., 2010).

The isotope composition will be expressed in the δ notation (‰; g/kg). This notation expresses the D/H ratio of the sample (R_{sample}) relative to the D/H ratio of the Vienna Standard Mean Ocean Water ($R_{standard}$; $155,75.10^{-6}$) (Eq. 2.9) (Schwendenmann et al., 2010).

$$\delta^2 H = \left(\frac{R_{sample}}{R_{standard}} - 1\right).1000 \tag{2.9}$$

Prior to the experiment plant petioles, stem and soil were covered with aluminum foil (Figure 2.12). The mini HFD-sensor was only wrapped with aluminum foil and not with bubble wrap in order to be able to cut up plants more quickly during the experiment. For the same reason only aluminum foil was used and no tape for coverage. Leaves were bent downward and partially covered with aluminum foil in order to avoid contamination by a downward flow at the edge of the leaves.

The protocol used for assessing hydraulic redistribution commences with a control experiment. Three control plants were sprayed with tap water for 1 h, from 9.30 - 10.30 am, DOY 125. After spraying, plants were immediately cut in various pieces: leave blades, petioles and stems. Leaves were separated in horizontal layers of upper, middle and lower leaves. Only one of the control plants had middle leaves. Individual pieces were patted dry and conserved in enclosed test tubes which were placed in a freezer. The subsequent day, DOY 126, leaves of four other plants were sprayed with heavy water (3020.85 $\pm$ 5.80 ‰ $\delta^2 H$). This is maintained for 1 h, from 9.40 - 10.40 am. In order to evaluate the redistribution pattern plants were immediately cut in various pieces: leave blades, petioles and stems. Leaves were separated in horizontal layers of upper, middle and lower leaves. Individual pieces were patted dry and conserved in enclosed test tubes. Firstly the samples were

frozen for 24 hours. Secondly water was extracted from the sub-samples by cryogenic vacuum distillation with a vial thermo-reactor (HI 839800, Hanna Instruments, Woonsocket, United States of America) at 95 °C and salty ice water (Figure 2.13). Thirdly the isotope analysis was carried out with an isotopic water analyzer (L2120-i, Picarro, Santa Clara, United States of America).

Figure 2.12: Plant with stem, petioles and soil covered in aluminum foil. Leaves bent downward and partially covered with aluminum foil in order to avoid contamination.

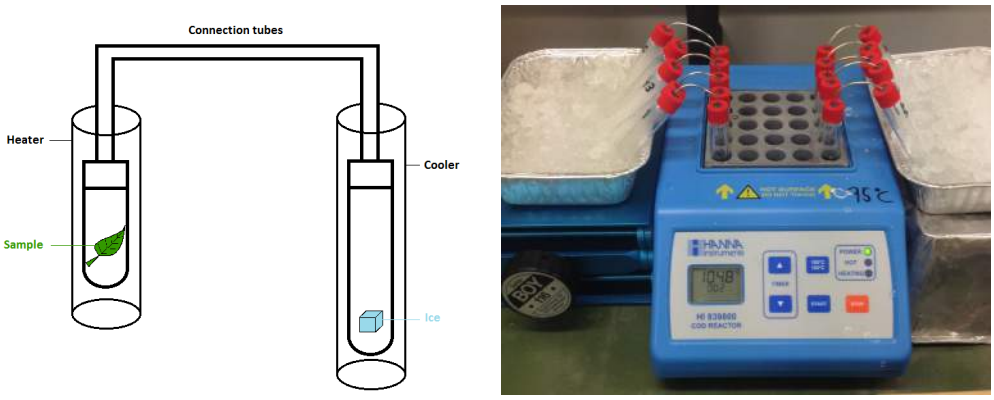

Figure 2.13: Set-up for cryogenic vacuum distillation. The frozen sample is placed in a heater, water sublimates out of the sample and deposits in the collection tube in a cooler with salty ice water. Left: Schematic set-up. Right: Set-up with heater in the middle and salty ice water at the left and the right of the heater.

A bottleneck in terms of analysis time is the extraction of water. In order to avoid fractionation, theoretically, all water should be extracted. However, West et al. (2006) indicated that the extraction could be significantly reduced without changing the isotope signature. Times indicated were 60-75 minutes for stems, 20-30 minutes for leaves and 30 minutes for sandy soils. However, out of precaution and due to low amounts of water present, for example in the petioles, the extraction was maintained for 4 hours. After the extraction oven drying took place at 105 $^{\circ}C$ for 48 hours.

Redistribution per plant organ can be expressed as a percentage of the total amount of water found in the respective organ originating from FWU of deuterated water (N [%]). These values can be assessed through a mass-balance of both the control and the deuterium experiment, resulting in following equation:

$$N = \frac{\delta^2 H_{sample} - \delta^2 H_{control}}{\delta^2 H_{spray} - \delta^2 H_{tap}}.100 \tag{2.10}$$

With $\delta^2 H_{sample}$ the $\delta^2 H$ of the deuterated sample, $\delta^2 H_{control}$ the $\delta^2 H$ of the respective control sample, e.g. the control of stems was used for the sample of stems, $\delta^2 H_{spray}$ the $\delta^2 H$ of the deuterated spraying water (3020.85 $\pm$ 5.80 ‰) and $\delta^2 H_{tap}$ the $\delta^2 H$ of the control spraying water or tap water (-60.80 $\pm$ 0.57 ‰).

The amount of water taken up per plant organ ($Uptake_d$ [g]) can be subsequently calculated as:

$$Uptake_d = \frac{(Mass_{wet} - Mass_{dry}).N}{Q.100} \tag{2.11}$$

With $Mass_{wet}$ [g] mass of the sample prior to the cryogenic vacuum distillation, $Mass_{dry}$ [g] the mass after oven drying and Q the number of plant parts in the respective sample. Q values for leaves are 2, for petioles 6 and for stems 1. In other words, there were 2 leaves in 1 sample, 6 petioles in 1 sample and 1 stem in 1 sample.

Chapter 3

Results

3.1 Experimental set-up

3.1.1 Biotic parameters

As a result of transport the epicotyl of some germinating seeds died off, most likely as a result of dehydration. However, in three seeds the formation of a secondary epicotyl was observed.

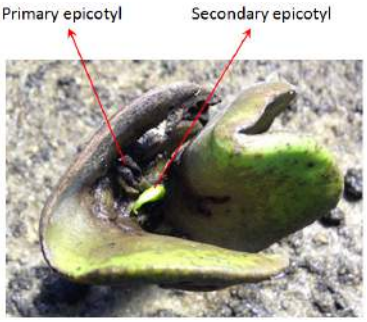

Figure 3.1: Primary and secondary epicotyl of an *A. marina* seedling.

3.1.2 Abiotic parameters

Micro-climate was characterized during all treatments and control phases by measuring the relative humidity (RH [%]), temperature (T [$^{\circ}C$]) and photosynthetically active radiation (PAR [$\mu mol.m^{-2}s^{-1}$]) and calculating the vapor pressure deficit (VPD [kPa]) (Figure 3.2 and 3.3). Abiotic parameters were similar for all plants with some small variation, for example, due to positioning relative to the lamps.

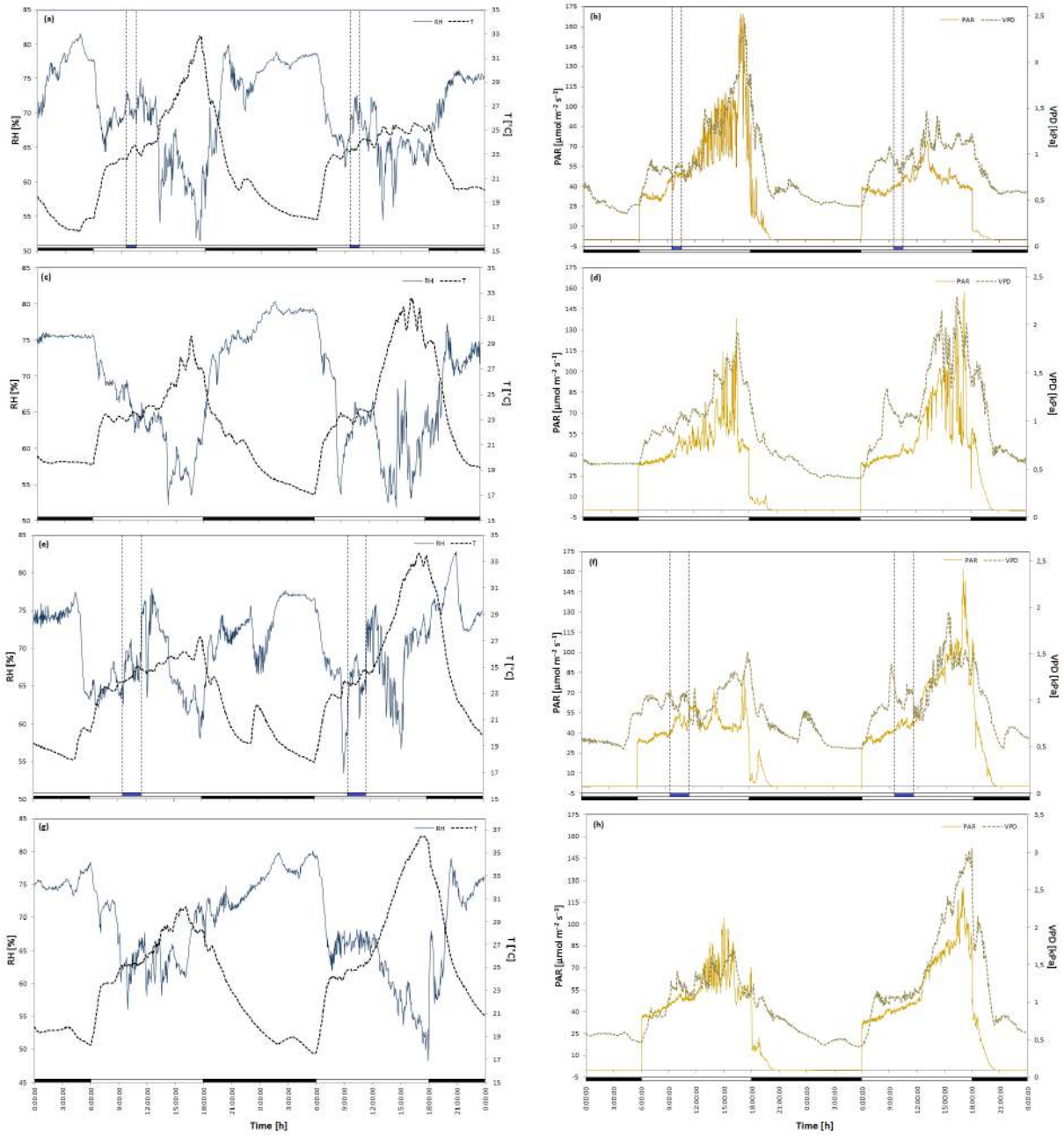

Figure 3.2: Relative humidity (RH; average of 2 measurements), temperature (T; average of 2 measurements), photosynthetic active radiation (PAR) and vapor pressure deficit (VPD) as a function of time. (a) and (b) day of the year (DOY) 92-93 (sap flow experiment 1; artificial rain events of 1 h), (c) and (d) DOY 94-95 (sap flow control 1), (e) and (f) DOY 96-97 (sap flow experiment 2; artificial rain events of 2 h), and (g) and (h) DOY 98-99 (sap flow control 2). Blue bars delimited by vertical dotted lines indicate an artificial rain event. White and black bars at the bottom indicate, respectively, when artificial lights are on and off.

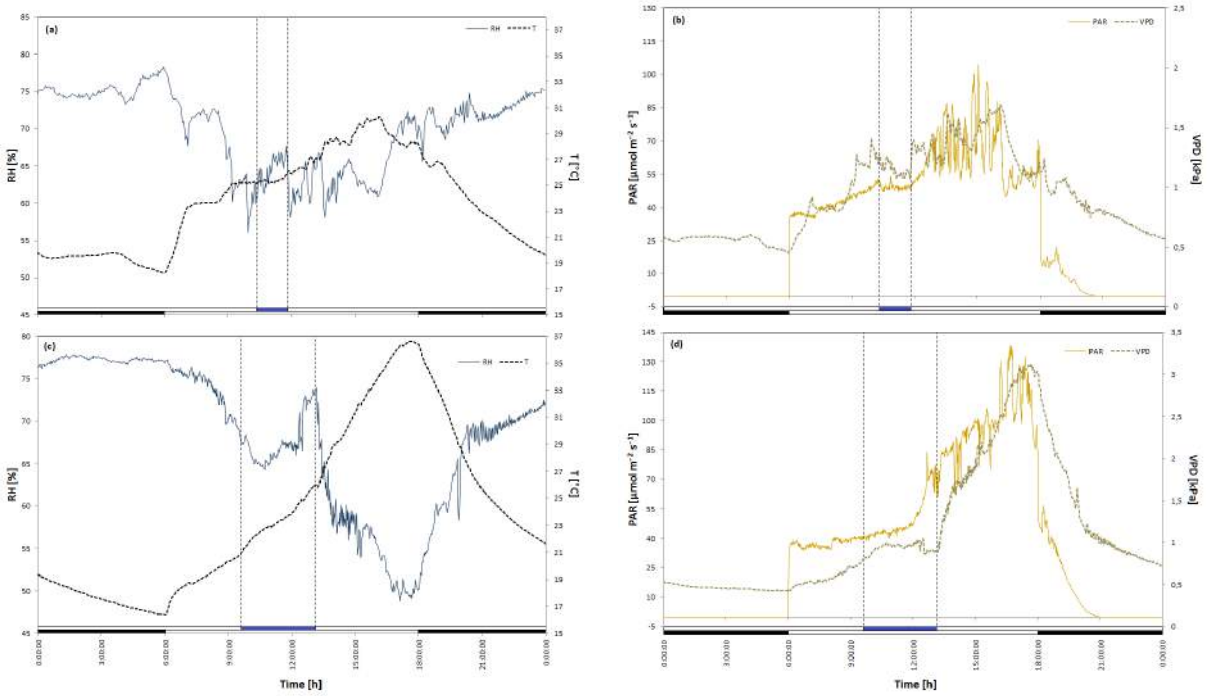

Figure 3.3: Relative humidity (RH; average of 2 measurements), temperature (T; average of 2 measurements), photosynthetic active radiation (PAR) and vapor pressure deficit (VPD) as a function of time. (a) and (b) day of the year (DOY) 98 (water potential experiment 1), (c) and (d) DOY 113 (water potential experiment 2). Blue bars delimited by vertical dotted lines indicate an artificial rain event. White and black bars at the bottom indicate, respectively, when artificial lights are on and off.

Overall RH ranged between $65 - 80$ % during nighttime and between $50 - 65$ % during daytime, seldom decreasing below 50, % excluding the effects of artificial rain events. T ranged roughly from $17 - 25$ $°C$ during nighttime and from $21 - 35$ $°C$ during daytime, following the inverse of the RH pattern. However, during and just after an artificial rain event the RH and T were decoupled resulting in an increase in RH independent of T.

PAR reacts strongly as the lamps are turned on and off at 6 am and 6 pm, respectively. In the morning variation in PAR is low due to the small amount of natural sunlight. In the afternoon this effect gets stronger. After turning off the lamps at 6 pm, PAR stays significantly larger than zero for a few hours due to natural sunlight.

VPD follows a similar pattern as PAR and T. However, VPD partially decouples during artificial rain events resulting in a decrease or stabilization of VPD, depending on the day, independent of PAR.

3.2 Sap flow

SF was measured using a mini HFD-sensors (Figure 3.4). During control days, the relative SF measurements followed a hump-shaped pattern indicating a positive SF during daytime and a relatively constant zero SF during nighttime. Patterns of this relative SF are similar to patterns of PAR, VPD and T. During artificial rain events SF decreased however substantially indicating a negative SF. The first event of the first treatment caused a small negative SF whereas the second event caused a large negative SF. Both events of the second treatment showed decreases in SF which were intermediate compared to the negative SF during the first treatment. Longer leaf wetting events during the second treatment resulted in a longer negative SF after leaf wetting has stopped compared to the negative SF of the first treatment.

First SF was expressed in function of VPD (Figure 3.5), excluding the artificial rain events. During nighttime there was no clear correlation between SF and VPD ($R^2 = 0.02$). During daytime this correlation was significantly higher, indicating that SF increased with VPD, until a maximum was reached. However correlation was still relatively low ($R^2 = 0.47$). Second, SF was expressed as a function of PAR (Figure 3.6). Correlation was high with an exponential curve ($R^2 = 0.75$), indicating that SF increased with PAR until a maximum was reached. Third SF was expressed in function of VPD and PAR (Figure 3.7). This relationship indicates that SF only rose with an increase in VPD when VPD was below 1.5 kPa. The data in this Figure displays measurements between 6 am and 6 pm. As such the data points in the absence of PAR were removed, seemingly minimizing the initial increase in SF for an increase in VPD. However, if these data points were included the overview of the other data points was not clear. In addition, Figure 3.5 has already shown that the correlation between SF an VPD is poor during nighttime. In Figure 3.7, however, it is clear that if VPD increases above the threshold of 1.5 kPa, SF starts to decrease again. The relationship between PAR and SF is the same as in Figure 3.6.

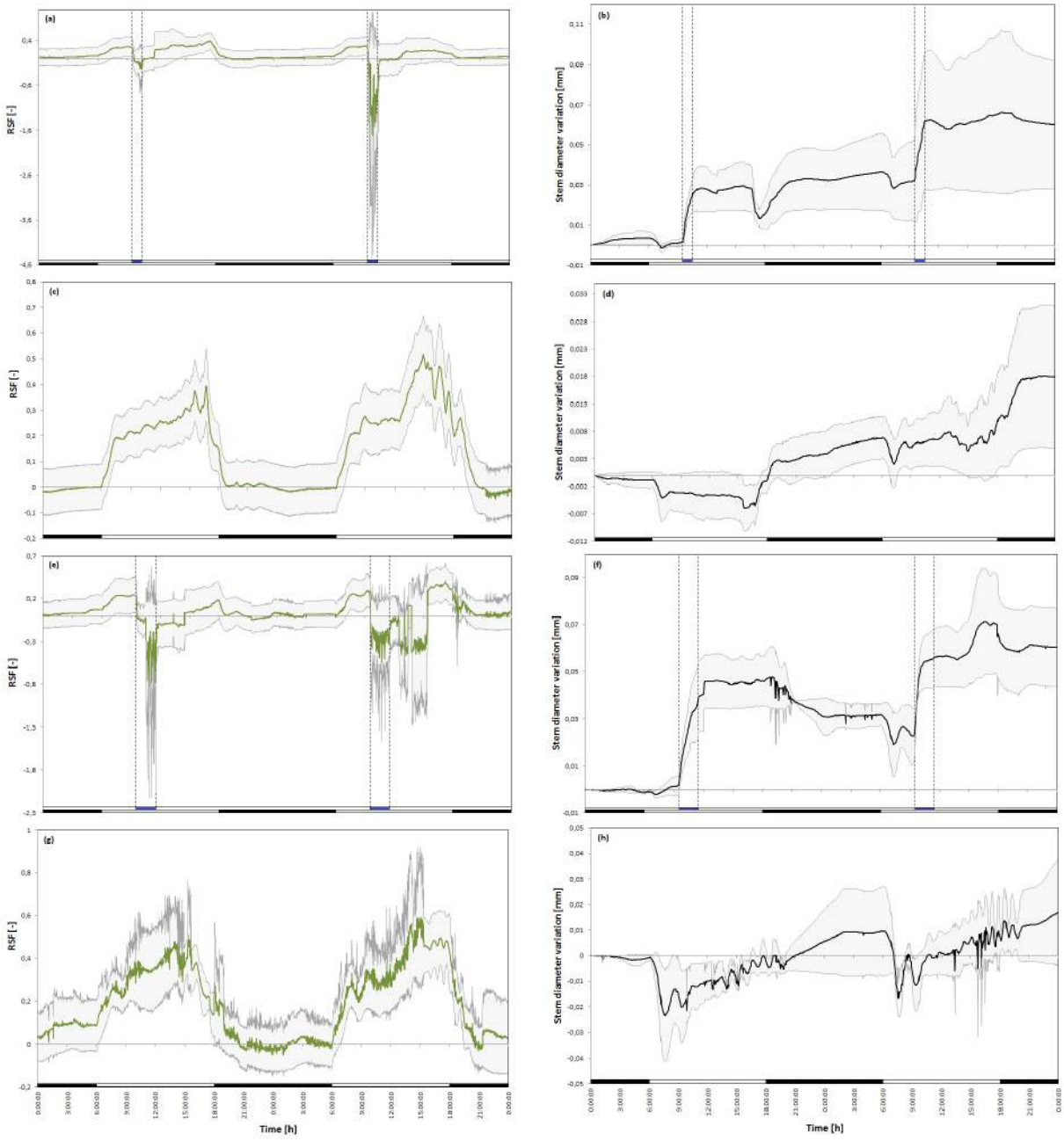

Figure 3.4: The HFD-ratio (RSF; average of 4 measurements) and stem diameter variation (average of 3 measurements, set to zero at the start of every 2 day measurement campaign) as a function of time. Grey lines indicate average ± standard deviation. (a) and (b) day of the year (DOY) 92-93 (experiment 1; artificial rain event of 1 h), (c) and (d) DOY 94-95 (control 1), (e) and (f) DOY 96-97 (experiment 2; artificial rain event of 2 h) and (g) and (h) over DOY 98-99 (control 2). Blue bars delimited by vertical dotted lines indicate an artificial rain event. White and black bars at the bottom indicate, respectively, when artificial lights are on and off.

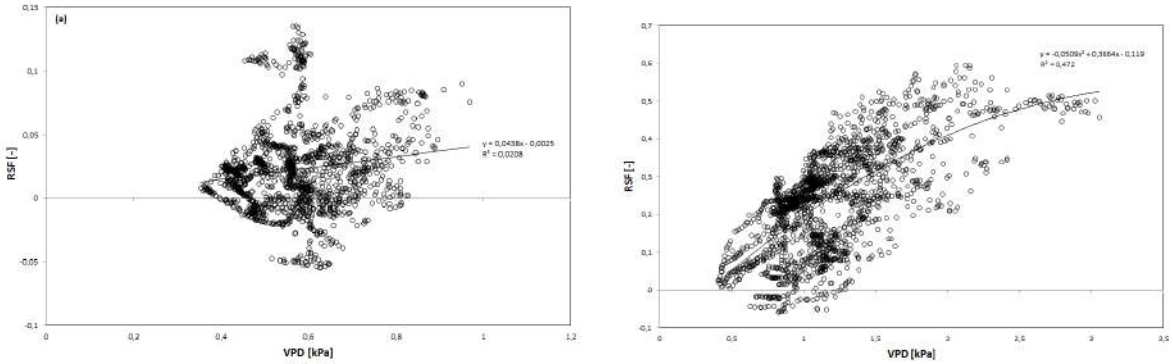

Figure 3.5: (a) Relationship between nighttime HFD-ratio (RSF; average of 4 measurements) and vapor pressure deficit (VPD) measured between 8 pm and 6 am over day of the year (DOY) 92-99. (b) Relationship between daytime HFD-ratio (RSF; average of 4 measurements) and vapor pressure deficit (VPD) measured between 6 am and 8 pm over DOY 92-99 (measurements during artificial rain events were excluded: DOY 92 from 9.30-12 am, DOY 93 from 9.30-12 am, DOY 96 from 9.30 am - 2.30 pm and DOY 97 from 9.30 am - 3.30 pm).

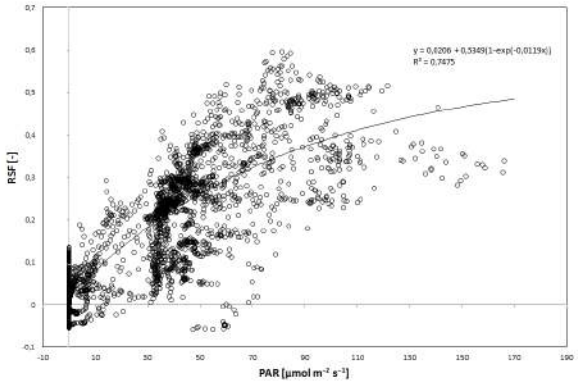

Figure 3.6: Relationship between HFD-ratio (RSF; average of 4 measurements) and photosynthetically active radiation (PAR) measured over day of the year (DOY) 92-99 (measurements during artificial rain events were excluded: DOY 92 from 9.30-12 am, DOY 93 from 9.30-12 am, DOY 96 from 9.30 am - 2.30 pm and DOY 97 from 9.30 am - 3.30 pm).

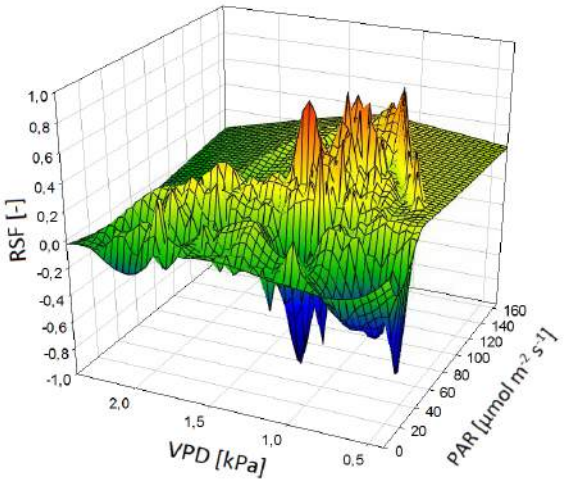

Figure 3.7: Relationship between HFD-ratio (RSF; average of 4 measurements), vapor pressure deficit (VPD) and photosynthetically active radiation (PAR) measured between 6 am and 6 pm over day of the year (DOY) 92-99 (measurements during artificial rain events were excluded: DOY 92 from 9.30-12 am, DOY 93 from 9.30-12 am, DOY 96 from 9.30 am - 2.30 pm and DOY 97 from 9.30 am - 3.30 pm). Planes in background or not real measurements but artificial completed trends, as is the data point with coordinates (0,0,0).

3.3 Stem diameter variation

SDV was measured using an LVDT-sensors (Figure 3.4). During control experiments stem diameters stayed relatively constant with small decreases during daytime and small increases during nighttime. After two days, a net increase of approximately 0.02 mm was measured during both control treatments. During artificial rain events diameters increased drastically followed by a small decrease. The net result is an increase in diameter of approximately 0.06 mm after two days for both experiments with one treatment per day. During the first experiment, stem diameter increased over the whole time range during both treatments. For the second sap flow experiment this was only the case for the first treatment. During the second treatment diameter increase was initially similar compared to the other experiments. Prior to the end of the treatment, the stem diameter increase slowed down substantially.

When expressing SDV in function of SF a linear correlation was found for the first treatment of both experiments (Figure 3.8; $R^2 = 0.82$ and 0.77 for the first and second experiment, respectively). For the second treatment of both experiments, SF and SDV correlated poorly ($R^2 = 0.28$ and 0.24 for the first and second experiment, respectively).

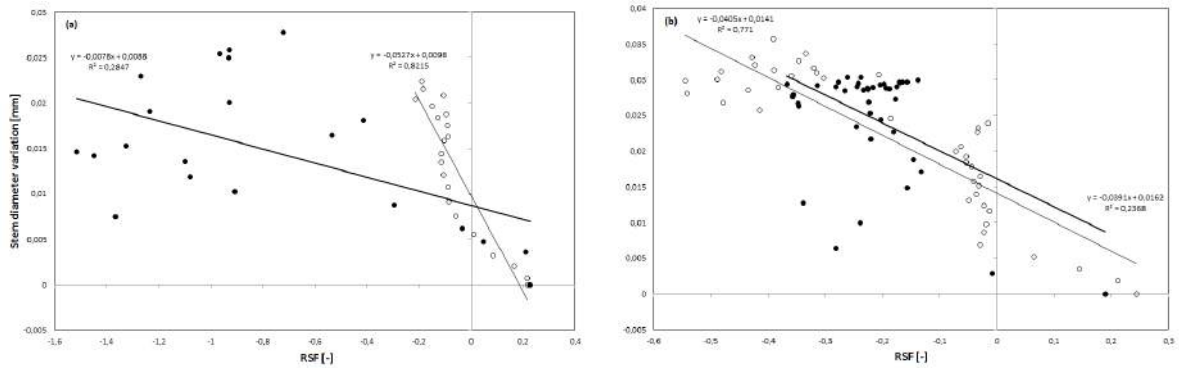

Figure 3.8: Relationship between HFD-ratio (RSF; average of 4 measurements) and stem diameter variation (average of 3 measurements) during the artificial rain events. Open symbols represent the first event of an experiment, filled symbols represent the second event of the same experiment. Stem diameter variation was set to zero at the start of every event. (a) Event 1 on day of the year (DOY) 92, event 2 on DOY 93 (experiment 1; artificial rain event of 1 h). (b) Event 1 on day of the year (DOY) 96, event 2 on DOY 97 (experiment 2; artificial rain event of 2 h).

3.4 Water potential

Measurements for Ψ of the irrigation water ranged from -1.64 to -1.84 MPa, which is lower than theoretically expected.

Ψ_{leaf} was measured prior, during and after two artificial rain events (Figure 3.9). Prior to the artificial rain event Ψ_{leaf} ranged from -6 to -3 MPa. When the artificial rain event started Ψ_{leaf} quickly rose until it reached a value of approximately -1.8 MPa, approximating the water potential of the irrigation water, where it stopped increasing and fluctuated around this value. When the artificial rain event stopped, Ψ_{leaf} decreased but slower than the initial increase.

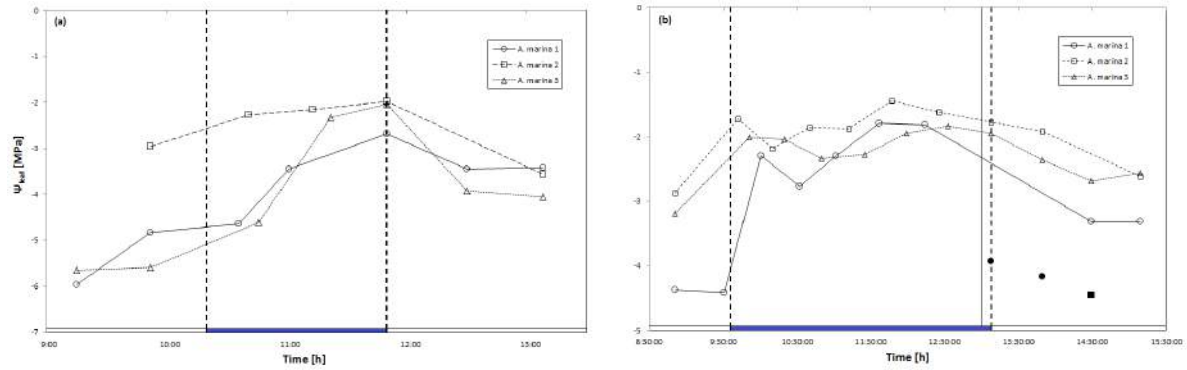

Figure 3.9: Water potential of leaves (Ψ) as a function of time during an artificial rain event. Blue bars delimited by vertical dotted lines indicate an artificial rain event. (a) Water potential experiment 1 during day of the year (DOY) 98. Tidal simulation was postponed at 1 pm until after the experiment. (b) Water potential experiment 2 during DOY 113. Vertical line indicates opening of the valve system at 1 pm for tidal simulation. Filled symbols represent outliers.

3.5 Foliar uptake capacity experiment

The water uptake of leaves per unit of area was assessed for old and young leaves through a 3 hour submergence test. One old leaf was labeled as an outlier and removed from the dataset. Young leaves had an average uptake of 0.01 g or 0.0012 $g.cm^{-2}$. The uptake of old leaves fluctuated around zero, with some negative values. As a consequence, only the ΔLWC [%] for young leaves was different from zero and approximated 0.4 % indicating FWU.

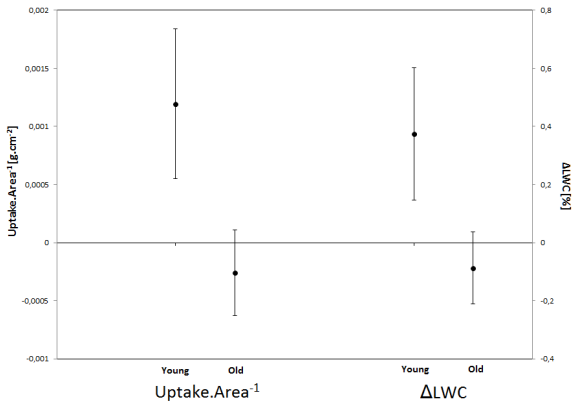

Figure 3.10: Average water uptake per unit of leaf area after submergence for 3 hours and average difference in leaf water content (LWC) for leaves before and after a 3 hour submergence. Leaves are separated in old (lower leaves, approximately 3-4 months old) and young (middle and upper leaves, approximately a few weeks to 2 months old) leaves. Vertical lines indicate the standard deviation of the average.

3.6 Hydraulic redistribution

During the deuterium experiments the relative SF was additionally measured (Figure 3.11). A negative SF was measured during the deuterium experiment, indicating that heavy water was taken up through the leaves.

When addressing the deuterium data a decreasing trend can be seen in δ^2H from contact point (leaves), to more distant features such as petioles and stems (Figure 3.12). However, all values of the deuterium experiment are high compared to the control samples. Remarkable is the larger concentration in the upper leaves compared to middle and lower leaves. In the most extreme case the δ^2H value of the upper leaves was five times higher than the δ^2H value of middle and lower leaves (data not shown per plant). The same trend can be seen in the percentage of water in the respective plant organ, originating from FWU (Figure 3.13). When assessing the total amount of deuterated water taken up per plant organ, this trend fades. The petioles contain too little water to maintain a similar trend.

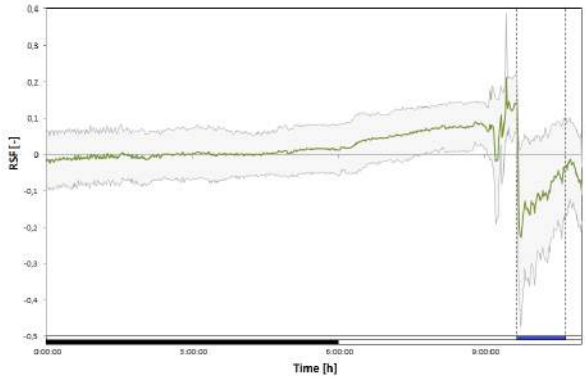

Figure 3.11: The HFD-ratio (RSF; average of 4 measurements) as a function of time over day of the year (DOY) 125. Grey lines indicate average ± standard deviation. Blue bars delimited by vertical dotted lines indicate an artificial rain event with deuterated water (3020.85 ± 5.80 ‰ δ^2H). White and black bars at the bottom indicate, respectively, when artificial lights are on and off.

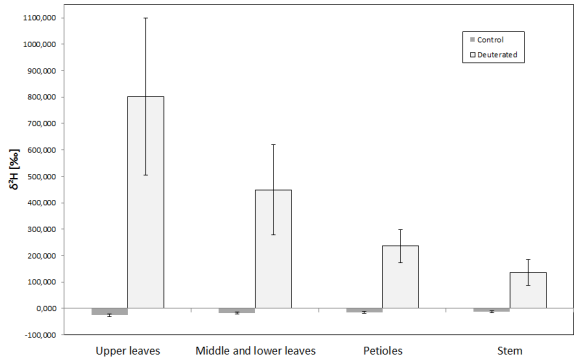

Figure 3.12: δ^2H values for different plant organs after the deuterium experiment and after control. Leaves were horizontally divided in sub samples. Control values are the average of 3 plants. Only 1 out of 3 control plants had middle leaves. Control samples were divided as follows: 6 upper leaves divided in 3 samples (1 sample per plant), 8 middle and lower leaves divided in 4 samples (1 sample per plant for lower leaves, 1 sample for middle leaves), 14 petioles divided in 3 samples (1 sample per plant) and 3 stems divided in 6 samples (2 sample per plant). Deuterated values are the average of 4 plants. Deuterated samples were divided as follows: 8 upper leaves divided in 4 samples (1 sample per plant), 16 middle and lower leaves divided in 8 samples (1 sample per plant for lower leaves, 1 sample per plant for middle leaves), 24 petioles divided in 4 samples (1 sample per plant) and 4 stems divided in 4 samples (1 sample per plant). 1 petiole, 1 stem and 1 lower leaf sample of the deuterated plants were rejected due to an insufficient extraction. Vertical lines indicate the standard deviation of the average.

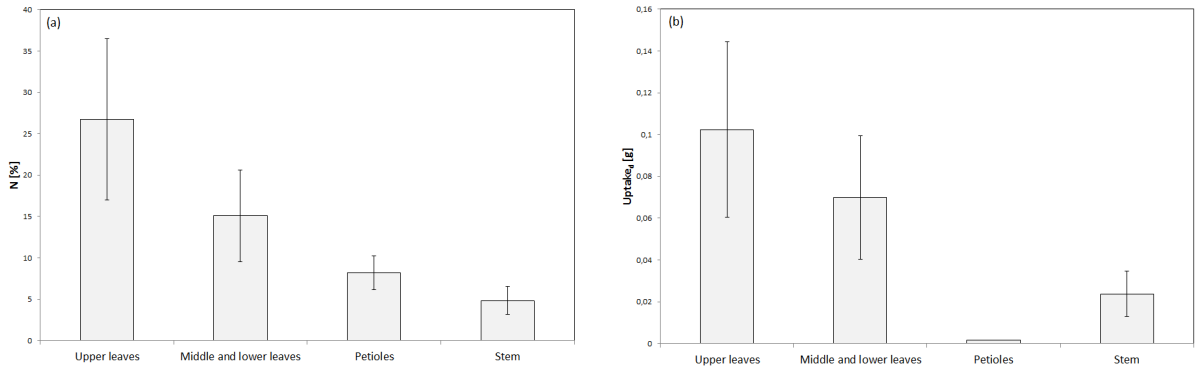

Figure 3.13: Water found in the respective plant organ resulting from foliar water uptake (FWU) of plants treated with deuterated water. Leaves were horizontally divided in sub samples. Values are the average of 4 plants. Samples were divided as follows: 8 upper leaves divided in 4 samples (1 sample per plant), 16 middle and lower leaves divided in 8 samples (1 sample per plant for lower leaves, 1 sample per plant for middle leaves), 24 petioles divided in 4 samples (1 sample per plant) and 4 stems divided in 4 samples (1 sample per plant). 1 petiole, 1 stem and 1 lower leaf were rejected due to an insufficient extraction. Vertical lines indicate the standard deviation of the average. (a) Percentage of the total amount of water found in the respective organ originating from FWU of deuterated water (N). (b) Amount of water found in the respective organ originating from FWU of deuterated water ($Uptake_d$).

Chapter 4

Discussion

4.1 Seedling survival

Physical disturbance by tidal inundation and sediment dynamics has been known as the bottleneck for mangrove seedling establishment. When sea-level rises due to climate change, establishment of mangrove seedlings might even get harder (Balke et al., 2015). However, the observed formation of a secondary epicotyl might indicate a larger resilience than previously thought (Figure 3.1). As such, when the propagule starts to germinate and environmental conditions get unfavorable, the propagule might get another establishment chance later on. This feature should be further assessed in terms of frequency of occurrence and time endured between conditions which induce primary and secondary epicotyl formation.

4.2 Growth

Liquid water is essential as a medium for metabolism, transport and growth. When assessing the Lockhart equation (Eq. 1.5) growth can occur when turgor exceeds a threshold value. This occurs due to the uptake of water. When FWU occurred, the stem diameter increased implying that turgor indeed exceeded the threshold in both sap flow experiments (Figure 3.4).

The strong negative correlation between SF and stem diameter variation during the first treatment of both sap flow experiments indicates that a negative SF due to FWU resulted in an increase in stem diameter (Figure 3.8). The difference in correlation between the first and second treatment of both sap flow experiments might be explained by a difference in the use of water taken up by FWU. It is expected that both rehydration of vascular tissue and the formation of new cells occur during both treatments of both events but possibly in a different proportion. It has been stated by Reef & Lovelock (2014) that the utilization of freshwater, when available, can increase mangrove survivorship, growth and productivity. Concomitant with our observations, this leads to the conclusion that FWU results in an increase in stem diameter or growth.

During the second artificial rain event of the second sap flow experiment diameter increase decreased drastically prior to the end of the experiment implying that turgor had reached a maximum. From our data it cannot be concluded that the maximal diameter increment, and hence growth, was reached during the first sap flow experiment. However, due to the fact that both sap flow experiments had a similar average increment of 0.03 $mm.day^{-1}$ and that during the second event of the second experiment probably a maximum increase in diameter was reached after 0.5 hours of the second artificial rain event, or 2.5 hours in total over the two days, it can be assumed that during the first experiment with a total duration of artificial rain events of 2 hours over 2 days a maximum of diameter increment was reached or approximated. From this it can be concluded that an average of 1 hour of precipitation per day could lead to maximal growth for *A. marina* saplings. Fully grown trees on the other hand should have larger hydraulic capacities, implying that a longer precipitation event would lead to a larger diameter increment. Nonetheless, with the methods used, radial increment due to water uptake by vascular tissue or formation of new cells cannot be distinguished (Robert et al., 2014). Due to the fact that the environmental conditions were kept constant and that no large diameter decreases occurred during this study, irreversible growth can be expected, following rehydration of the vascular tissue. Additionally, no large increment in diameter was measured in absence of an artificial rain event, suggesting that freshwater supplied by these events is crucial in order to induce and maintain a significant permanent growth for *A. marina*.

These average growth rates of 0.03 $mm.day^{-1}$ are high compared to the average diameter increments during the control days of 0.01 $mm.day^{-1}$ for both control periods, especially when taking into account the physiological drought stress that these trees have to endure due to salt in the irrigation water and the small circumference of the saplings (approximately 12.5 mm in circumference). In comparison, fully established peach trees are known to have a diameter growth rate of approximately $0.04 - 0.06$ $mm.day^{-1}$ during well watered conditions in the growing season (Garnier & Berger, 1986; Huguet et al., 1992) and different bamboo species have an average and maximal diameter growth rate of 0.06 $mm.day^{-1}$ and 0.13 $mm.day^{-1}$ respectively during the first year after planting (Kibwage et al., 2008). The well watered peach trees should be in a constant state of hydration which implies that turgor would almost constantly exceed the threshold value of growth during the night. This again highlights the magnitude of growth for *A. marina* during these artificial rain events. It can therefore be stated that precipitation is of primary importance for the increase of turgor above the threshold of growth for *A. marina*. Without precipitation growth will decrease drastically or may even come to a halt as has been observed by Santini et al. (2015) (Figure 4.1). They found no significant diameter increment for *A. marina* in the absence of precipitation on two different measuring sites. This coincides with the statements of Spalding et al. (1997) and Clough (2013) that the distribution of mangrove communities is more limited by rainfall and aridity than by air temperature. Robert et al. (2014) stated that radial increment of *A. marina* is more affected by the availability of fresh water, e.g. precipitation, than by tidal inundation. However, results in this paper stated an annual diameter increment of approximately 2 mm or 0.005 $mm.day^{-1}$ and a

maximal diameter increment of 0.09 $mm.day^{-1}$ during a rainy day for an *A. marina* tree with a circumference of 130 *cm*. These values are low compared to our measurements, when taking the circumference into account. It is suggested, however, that the large increase in diameter during rain events is caused by freshwater availability, implying freshwater at the root level caused this increment. We suggest that this is incomplete as water is also taken up at the leaf level which additionally results in an increase of water uptake and a decrease in water loss due to the suppression of transpiration.

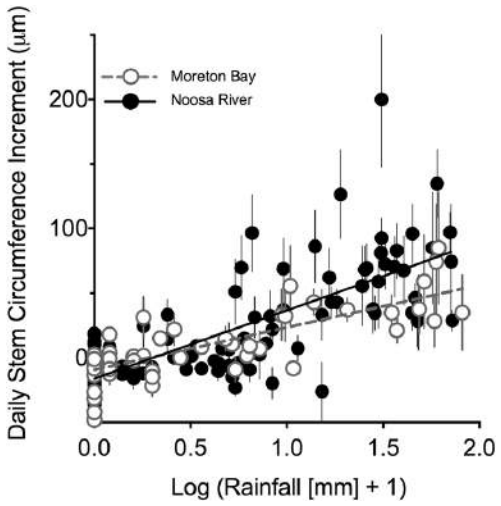

Figure 4.1: Relationship between daily stem circumference increment and Log (Rainfall [mm] + 1). For Moreton Bay, the regression is: $Increment = 34.Log(Rainfall[mm] + 1) - 10.5$ ($R^2 = 0.34$) and for the Noosa River, the regression is: $Increment = 62.Log(Rainfall[mm] + 1) - 20$ ($R^2 = 0.37$) (Santini et al., 2015)

It has been stated by Niglas et al. (2014) that Ψ_{soil} is a more significant factor influencing tree growth than RH. Nonetheless, a decrease in SF due to an increase in RH might limit nutrient uptake, thus limiting growth. If precipitation increase due to climate change, RH would increase during these events possibly restricting growth (Kupper et al., 2010). In this study FWU during artificial rain events resulted in a irreversible increase in diameter. This confirms the statement of Santini et al. (2015) that growth of *A. marina* benefits from an increase in fresh water availability, especially when salinity supersedes the optimum range for *A. marina* of 3.5-17.5 ‰ which is the case in this study (salinity of 19.6 ‰).

4.3 Sap flow and foliar water uptake

The driving force for transpiration is the difference between the actual water vapor pressure in the air, depending on RH and T, and in the leaf interior, depending on leaf temperature (T_{leaf}) and water availability. During a leaf wetting event RH increases and T_{leaf} and VPD decrease due to evaporation (Kupper et al., 2010). While it has been reported that an

elevated RH can result in a higher stomatal conductance and an increased transpiration, most findings suggest that a higher RH results in a lower SF (Niglas et al., 2014). This is confirmed by the statement of Eller et al. (2015) that leaf-wetting events have a strong suppressive effect on the transpiration of trees. FWU does not only lead to water gain for the plant, but also reduces water loss by transpiration (Eller et al., 2015). In the absence of a an artificial leaf wetting event in our experiments, radiation due to lamps and natural sunlight led to an increase in T and VPD and a decrease in RH (Figure 3.2 and 3.3). However, VPD and RH are also dependent on the total availability of water in the greenhouse. This was not a problem, given the presence of two humidifiers. It might be stated that variation in PAR is the driving force for variation in T, RH and VPD through changes in T and RH. When plants are not subjected to drought stress they open their stomata when subjected to PAR. This explains the high correlation between SF and PAR (Figure 3.6). As a result of radiation, VPD increases resulting in a larger 'water demand' of air followed by an increase in transpiration. However, as VPD becomes larger, plants start to close their stomata resulting in a decreasing SF (Figure 3.7). In our data we found that SF started to decrease above a VPD of 1.5 kPa. It can be stated that a high VPD decreases stomatal conductivity leading to a stabilization in SF (Paudel et al., 2015). Given the poor correlation between VPD and SF during nighttime it can be concluded that a good stomatal closure occurred at night (Figure 3.5). This closure might be caused by two factors: first leaf-wetting as a result of a higher RH at night and second an increased sensitivity of stomatal conductance to changes in VPD and soil water content during nighttime. These later adaptations might occur in order to reduce water loss when carbon assimilation is absent (Eller et al., 2015). During daytime the correlation between SF and VPD was significantly higher due to the link between transpiration, VPD and stomatal opening. This indicates the strong interaction between stomatal control and the abiotic environment (Paudel et al., 2015). During artificial rain events VPD partially decoupled and decreased or stabilized, depending on the day, independent of PAR. The partial decoupling of VPD would not occur in natural conditions.

As a result of the increased RH and the direct water contact with leaves during artificial rain events, a negative SF was measured concomitant with an increase in stem diameter. Leaf wetting events can slow down or prevent transpiration (Burns et al., 2009), however the negative SF and increase in stem diameter suggests that also FWU occurred. Stems and petioles were covered with aluminum foil and tape in order to prevent water uptake by other organs resulting in a negative SF. However, tissue dehydration (TD) could also result in a negative SF, but during artificial rain events Ψ_{leaf} increased to approximately the same value as Ψ of the irrigation water indicating a hydraulic equilibrium between irrigation water and plant (Figure 3.9). TD cannot result in a large increase in Ψ_{leaf} simultaneously with a negative SF. FWU on the other hand results in an immediate increase in LWC and plant water potential (Burns et al., 2009), thus reinforcing the statement that SF caused by FWU is driven by a water potential gradient in the SPAC (Eller et al., 2015). It can be concluded that FWU took place resulting in a negative SF. However, measured Ψ of the irrigation water was lower than theoretically expected. This might be caused by dissolved

organic matter originating from the peat in the planting substrate. Nonetheless, FWU will lead to an enhanced gas exchange after leaves dry, a higher survival rate and an increased growth (Burns et al., 2009) as illustrated by the increment in stem diameter (section 4.2). The magnitude of FWU should increase with a dryer soil and a longer duration of the leaf-wetting event (Eller et al., 2015). As mangroves grow in a saline environment, they are always subjected to physiological drought. As such, this environment can be defined as favorable in terms of FWU. FWU might also cause embolism repair. However, as cavitation fatigue has not been assessed for *A. marina*, the importance of this repair cannot be fully accessed. The anatomical adaptations of mangroves to salinity such as the formation of smaller vessels in a higher density when salinity increases, reduces the risk of embolism formation. Larger vessels are formed when salinity decreases in order to increase hydraulic conductivity and concomitant carbon assimilation and growth (Reef & Lovelock, 2014).

Due to possible inaccuracy during manual measurements for Ψ, the hydraulic equilibrium between irrigation water and plants might not be reached resulting in a combined SF from root and leaves to stem if Ψ_{leaf} was lower than measured. If Ψ_{leaf} was higher than measured a complete reversal of the SPAC-flow is possible manifesting itself by a sap flow from leaves, through plant into the irrigation water. It does not seem likely that a combined SF from root and leaves took place due to the low placement of the HFD-sensor and the reverse SF measured. It can be concluded that at least a hydraulic equilibrium and possibly an efflux to the irrigation water took place.

The order of magnitude of the negative SF is large and on average approximates the same absolute value as the positive SF during the day. FWU of fog water in the tropical cloud forest species *Drimys brasiliensis* reached a negative SF during fog events up to 26 % of the maximal daily transpiration. This confirms the possible inversion of water movement through the SPAC due to water sources which cause a change in water potential (Steppe et al., 2015b). Our data confirm the findings of Oliveira et al. (2005) that a longer leaf wetting event results in a longer negative SF after the leaf wetting has halted. During the first sap flow experiment both treatments lasted 1 hour. Almost immediately after terminating the artificial rain event, negative SF stopped and 1.5 hours after the end of the artificial rain event a positive SF resumed the normal daily SF-pattern. During the second sap flow experiment both treatments lasted 2 hours. After stopping the artificial rain events a negative sap flow was maintained for approximately 3-4 hours. After this time span a positive SF resumed. All abiotic parameters were similar during both experiments. This implies that FWU occurs during the whole experiment, resulting in a high water potential in the upper parts which led to a hydraulic redistribution of water, even after the leaf wetting events had halted. However, due to the high humidity, leaves might have been able to hold water for a longer time after the artificial rain simulation had stopped.

When assessing the full extend of FWU an up-scaling needs to be done with additional data of leaf area index (LAI) and leaf longevity of *A. marina*. Laongmanee et al. (2013) reported a mean leaf area index of $2 - 3\ m^2_{leaves}.m^{-2}_{soil}$ for *A. marina* and Wang'ondu et al. (2010) stated that the average leaf longevity of *A. marina* was 9-11 months. When assum-

ing that the average foliar uptake capacity measured for young leaves of 0.0012 $g.cm^{-2}$ for *A. marina* (Figure 3.10) is universal for the first 2 months, we can calculate how much water is taken up through FWU per m^2 of *A. marina* forest. When maintaining an LAI of 2-3 while leaves only have an average longevity of 10 months, on average every 10 months leaves should be replaced. As such 2/10 leaves are 2 months old or younger. By multiplying this with an average LAI of 2.5 we get 0.5 $m^2_{leaves.young}.m^{-2}_{soil}$. By multiplying this result with 0.0012 $g.cm^{-2}_{leaves.young}$ or 12 $g.m^{-2}_{leaves.young}$ we get a possible FWU of 6 $g.m^{-2}_{soil}$ or 6 $g.m^{-2}_{forest}$. If stem water uptake by young shoots would be accounted for, the water uptake might increase significantly. Uptake is larger in trees in natural conditions due to the fact that water can be redistributed from the leaves to other organs making the leaf accessible to a renewed water uptake. The larger uptake when leaves are attached to the plant has been confirmed by our hydraulic redistribution experiment (Figure 3.13; section 4.4). Additionally, some negative values were measured with the foliar uptake capacity experiment. This might have occurred due to small leaf particles that remained on the tape when removing leaves from the petri dishes. An alternative explanation could be that salt dissolved from the leaf surface into the water and resulted in a low Ψ_o of the submergence water resulting in water extraction from the sample. The latter seems very unlikely as leaves were patted dry and salt was removed on a visual basis prior to the experiment. The possible remaining quantity of salt on the leaf surface is therefore unlikely to be sufficient to lower Ψ_o of the submergence water enough as to extract water from the samples into the petri dishes. However, if leaf particles were stuck on the tape, this might also have been the case for other leaves with a positive water uptake. As such, FWU might have been underestimated. Nonetheless, the significance of FWU is variable through time as some seasonality was reported in respect to leaf longevity and LAI. It has also been stated by Eller et al. (2015) that nocturnal FWU is substantially larger than diurnal FWU.

In the study from Burns et al. (2009) FWU increased leaf water content in half of the investigated species by 2-11 % despite the fact that plants were well hydrated and the driving $\Delta\Psi$ across the leaf surface was small. This study also indicated that FWU may increase with moderate drought stress, until the pathway for absorption is restricted by dehydration. Burgess & Dawson (2004) stated that older leaves are better suited for FWU due to the occurrence of features such as cracks in the cuticle and general decay of the leaf surfaces or fungal hyphae conducting water into the stomata. Our data, however, suggest the inverse. Young leaves of *A. marina* appeared to be better suited for FWU contrary to older leaves. This might have occurred due to internal blockage of the FWU pathway as some necroses were observed on the older leaves. As such, the statement of Burgess & Dawson (2004) that up-scaling from measurements of one type of leaf cannot be done due to large variability in FWU between leaves of different ages and water statuses is confirmed. However, our conclusion with respect to leaf age is inverse for *A. marina* in contrast to the reported relationship by Burgess & Dawson (2004).

FWU enables plants to bypass water uptake through roots and benefit from most pre-

cipitation events, even when soil water potential is not substantially increased. This might be of primary importance as the frequency and intensity of extreme droughts is expected to increase due to climate change (Breashears et al., 2008).

4.4 Hydraulic redistribution

FWU leads to an immediate increase in plant water potential, resulting in at least a hydraulic equilibrium between *A. marina* and the irrigation water and possibly an efflux to the irrigation water. Both options imply that water is taken up by the leaves and redistributed to other organs or the soil and/or the irrigation water. The starting Ψ_{leaf} of both water potential experiments is quite different, despite the fact that the same plants were used for both experiments at the same hour of the day. This might be due to the fact that leaves used during the first experiment were upper and middle leaves, whereas the leaves used in the second experiment were middle and lower leaves. This difference occurred due to the limited amount of samples that can be taken from one leaf. The amount of water that was redistributed to each plant organ should depend on the total amount of water that the respective organ can hold (Figure 3.13). As the petioles only had small amounts of deuterated water it can be concluded that they can only hold small amounts of water. This seems plausible due to their small size. Our data also imply that redistribution first occurs to plant organs close to the point of uptake, in this case the leaves (Figure 3.12). The percentage of water originating from FWU in a plant organ decreases with distance from the leaves where uptake occured (Figure 3.13). However, patchiness occurs in *A. marina* as stated by Robert et al. (2014). As a consequence, FWU in fully grown trees could favor other organs, such as roots, resulting in smaller amounts of water left in the stem than would be expected.

As the upper, and by consequence, younger leaves take up more water it is assumable that stem parts close to the upper leaves received more water from FWU uptake then lower stem parts at an equal distance from lower leaves. However, the stem received a larger total amount of deuterated water then the petioles. This is due to their capacity to store more water. Nonetheless, it should be noted that the mini HFD-sensors were placed below the lower leaves. The negative SF measured is a result of FWU of all leaves subtracted with the amount of water which is taken up and redistributed to plant parts above the sensor. No nocturnal experiments took place. As such, the statement of Eller et al. (2015) that nocturnal FWU is substantially larger than diurnal FWU cannot be confirmed nor rejected for *A. marina*.

This experiment confirms the statement of Breashears et al. (2008) that the interpretation of plant water uptake through isotopic signatures must take FWU into account as the uptake of precipitation water might alter the isotopic signature substantially.

An increase in FWU when the leaf is still connected to the plant due to hydraulic redistribution has also been confirmed. When dividing the uptake of the leaves in the deuterium experiment by the area of the largest leaf in the foliar uptake capacity experiment, the upper leaves and middle and lower leaves have taken up 0.009 $g.cm^{-2}_{leaves.young}$ or 90 $g.m^{-2}_{leaves.young}$ and 0.006 $g.cm^{-2}_{leaves.old}$ or 60 $g.m^{-2}_{leaves.old}$, respectively. When retaking the calculations made for the foliar uptake capacity experiment we obtain 0.5 $m^2_{leaves.young}.m^{-2}_{soil}$ and 2.0 $m^2_{leaves.old}.m^{-2}_{soil}$. This leads to a combined FWU of 165 $g.m^{-2}_{soil}$ or 0.165 mm in 1 hour. The amounts of water transported to other organs is not taken into account, which means that the total amount of FWU per unit of area should still be higher. This amount is significantly larger than indicated by the foliar uptake capacity experiment. It can be concluded that the foliar uptake capacity experiment is good for indicating the possibility of FWU, but is a strong underestimation in terms of total FWU. Nonetheless, the foliar uptake capacity experiment confirmed that FWU does occur.

Chapter 5

Conclusion

The goal of this thesis work was to assess the link between foliar water uptake and growth of *Avicennia marina*, keeping in mind possible changes of precipitation patterns due to climate change. Several ecophysiological variables were measured such as sap flow, stem diameter variations and leaf water potentials prior, during and post artificial rain events. Hydraulic redistribution and abiotic parameters were recorded as well.

An increase in leaf water potential during artificial rain events indicated that water was taken up through leaves. This increase was rapid and came to a halt when a similar water potential was obtained as for the irrigation water, implying that a hydraulic equilibrium was reached.

A negative sap flow was measured during the artificial rain events, indicating that water was not only taken up by the leaves but was also redistributed in the plant. This led to a concomitant increase in stem diameter. No large decreases in stem diameter were measured during the entire experiment, indicating that the increase resulting from foliar water uptake was permanent. Additionally, no large increment in diameter was measured in absence of an artificial rain events, suggesting that freshwater supplied by these events is crucial in order to maintain a significant permanent growth for *Avicennia marina*. Hydraulic redistribution has been assessed through a deuterium experiment. This experiment confirmed that water was taken up by the leaves and redistributed to other plant organs. The first organs that were replenished were those close to the point of uptake, in this case the leaves. The foliar uptake capacity experiment proved that foliar water uptake occurred.

From this research it is shown that foliar water uptake is an important strategy to overcome long periods of physiological drought. Total amounts of redistributed water are relatively small. However, these amounts might be of primary importance to survive, particularly when climate change results in longer periods of drought. When small precipitation events occur, insufficient to significantly raise the water potential of the soil, enough water might be taken up by *A. marina* through foliar water uptake in order to survive. Even if climate does not undergo drastic changes in these areas, our data clearly shows

that precipitation and concomitant foliar water uptake is the primary driver for permanent growth of *A. marina*.

In conclusion, the hypothesis that *A. marina* could benefit from precipitation by foliar water uptake and thus could maintain growth in what would otherwise be unfavourable conditions is accepted.

Further research is needed in order to assess the full impact of climate change on the growth of *Avicennia marina*. Some other variables need to be investigated such as the effect of changing temperatures, changes in CO_2 concentration, changes in salinity and their interactions. When addressing foliar water uptake, stem water uptake should be excluded. This has not always been done in the past, but proved to be a contributing factor to water uptake in this work. In terms of establishment the formation of a secondary epicotyl should be examined in terms of frequency of occurrence and time endured between conditions which induce primary and secondary epicotyl formation. Finally, the possible improvement of the calibration of the mini HFD sensor should be assessed more in depth.

Bibliography

Abtew W. and Melesse A. 2013. Evaporation and evapotranspiration, Springer pp. 53-55

Balke T., Swales A., Lovelock C. E., Herman P. M. J. and Bouma T. J. 2015. Limits to seaward expansion of mangroves: Translating physical disturbance mechanisms into seedling survival gradients, Journal of experimental marine biology and ecology 467: pp. 16-25

Becker P., Asmat A., Mohamad J., Moksin M. and Tyree M. T. 1997. Sap flow rates of mangrove trees are not unusually low, Trees 11: pp. 432-435

Biasutti M. and Yuter S. E. 2013. Observed frequency and intensity of tropical precipitation from instantaneous estimates, Journal of geophysical research: atmospheres 118: p. 9534

Breshears D. D., McDowell N. G., Goddard K. L., Dayem K. E., Martens S. N., Meyer C. W. and Brown K. M. 2008. Foliar absorption of intercepted rainfall improves woody plant water status most during drought, Ecology 89(1): pp. 41-47

Burgess S. S. O. and Dawson T. E. 2004. The contribution of fog to the water relations of *Sequoia sempervirens* (D. Don): foliar uptake and prevention of dehydration, Plant, Cell and Environment 27: pp. 1023-1034

Burns E., Simonin K. A., Bothman A. G. and Dawson T. E. 2009 Foliar water uptake: a common water acquisition strategy for plants of the redwood forest, Oecologia (161): pp. 449-459

Campbell N. A., Reece J. B., Urry, L. A., Cain M. L., Wasserman S. A., Minorsky P. V. and Jackson R. B. 2008. Biology, Eight Edition, Pearson

Cardona-Olarte P., Krauss K. W. and Twilley R. R. 2013. Leaf gas exchange and nutrient use efficiency help explain the distribution of two Neotropical mangroves under contrasting flooding and salinity, International Journal of Forestry Research, Article ID 524625

Chapin F. S., Matson P. A. and Mooney H. A. 2002. Principles of Terrestrial Ecosystem Ecology, Springer

Clough B. 2013. Continuing the Journey Amongst Mangroves, ISME Mangrove Educational Book Series No. 1. International Society for Mangrove Ecosystems (ISME), Okinawa, Japan, and International Tropical Timber Organization (ITTO), Yokohama, Japan.

Crumbie M. C. 1987. *Avicennia Marina* - The Gray Mangrove, *http* : *//www.enhg.org/bulletin/b*32/32_02.*htm* - Accessed 31 October 2014

De Groote S., Steppe K. and Vandegehuchte M. 2013. Impact of dew and rain on water relations of the mangrove species *Avicennia marina* (Forssk.) Vierh., Ghent University, Master Thesis

De Swaef T., Hanssens J., Cornelis A. and Steppe K. 2012. Non-destructive estimation of root pressure using sap flow, stem diameter measurements and mechanistic modelling, Annals of Botany 111: pp. 271-282

Eller C. B., Lima A. L. and Oliveira R. S. 2013 Foliar uptake of fog water and transport belowground alleviates drought effects in the cloud forest tree species, *Drimys brasiliensis* (Winteraceae), New Phytologist 199: pp. 151-162

Eller C. B., Burgess S. S. O. and Oliveira R. A. 2015. Environmental controls in the water use patterns of a tropical cloud forest species, *Drimys brasiliensis* (Winteraceae), Tree Physiology 35: pp. 387-399

Elssworth P. Z. and Williams D. G. 2007. Hydrogen isotope fractionation during water uptake by woody xerophytes, Plant soil (291): pp. 93-107

Farrant J. M., Pammenter N. W. and Berjak P. 1993a. Seed development in relation to desiccation tolerance: A comparison between desiccation-sensitive (recalcitrant) seeds of *Avicennia marina* and desiccation-tolerant types, Seed Science Research 3: pp. 1-13

Farrant J. M., Berjak P. and Pammenter N. W. 1993b. Studies on the development of the desiccation-sensitive (recalcitrant) seeds of *Avicennia marina* (Forssk.) Vierh.: The acquisition of germinability and response to storage and dehydration, Annals of Botany 71: pp. 405-410

Forster M. 2014. Heat Ratio Method & Heat Field Deformation Method, *http* : *//ictinternational.com/content/uploads/*2014/05/$hrm - hfd - methods.pdf$ - Accessed 3 November 2014

Garnier E. and Berger A. 1986. Effect of water stress on stem diameter changes of peach trees growing in the field, Journal of Applied Ecology (23): pp. 193-209

Giri C., Ochieng E., Tieszen L. L., Zhu Z., Singh A., Loveland T., Masek J. and Duke N. 2011. Status and distribution of mangrove forests of the world using earth observation satellite data, Global Ecology and Biogeography 20: pp. 154-159

Goldsmith G. R. 2013. Changing directions: the atmosphere-plant-soil continuum, New Phytologist 199: pp. 4-6

Goldsmith G. R., Matzke N. J. and Dawson T. E. 2013. The incidence and implications of clouds for cloud forest plant water relations, Ecology letters 16: pp. 307-314

Hanssens J., De Swaef T., Nadezhdina N. and Steppe K. 2013. Measurement of sap flow dynamics through the tomato peduncle using a non-invasive sensor based on the heat field deformation method, Acta Horticulturae 991: pp. 409-416

Hogarth P. J. 2007. The biology of mangroves and seagrasses, Oxford University Press

Hubeau M., Vandegehuchte M. W., Guyot A., Lovelock C. E., Lockington D. A. and Steppe K. 2014. Plant-water relations of the mangrove species *Rhizophora stylosa*: a unique story, Communications in agricultural and applied biological sciences 79 (1): pp. 57-62

Huguet J. G., Lorendeau J. Y. and Pelloux G. 1992. Specific micromorphometric reactions of fruit trees to water stress and irrigation scheduling automation, Journal of Horticultural Science 67 (5): pp. 631-640

IPCC review editors: Aldunce P., Downing T., Joussaume S., Kundzewicz Z., Palutikof J., Skea J., Tanaka K., Tangang F. Wenying C. and Xiao-Ye Z. 2014. Climate change 2014: Synthesis report, IPCC Fifth Assessment Synthesis Report

Kibwage J. K., Netondo G. W., Odondo A. J., Oindo B. O., Momanyi G. M. and Jinhe F. 2008 Growth performance of bamboo in tobacco-growing regions in South Nyanza, Kenya, African Journal of Agricultural Research Vol. 3 (10): pp. 716-724

Kupper P., Sũber J., Sellin A., Lõhmus K., Tullus A., Räim O., Lubenets K., Tulva I., Uri V. Zobel M., Kull O. and S ober A. 2010 An experimental facility for free air humidity manipulation (FAHM) can alter water flux through deciduous tree canopy, Environmental and experimental botany 72: pp. 432-438

Lambs L. and Saenger A. 2011. Sap flow measurements of *Ceriops tagal* and *Rhozophora mucronata* mangrove trees by deuterium tracing and lysimetry, Rapid Communications in Mass Spectrometry 25: pp. 2741-2748

Lambers H., Chapin III F. S. and Pons T. L. 2008. Plant physiological ecology, Second Edition, Springer

Laongmanee W., Vaiphasa C. and Laongmanee P. 2013. Assessment of spatial resolution in estimating leaf area index from satellite images: a casae study with *Avicennia marina* plantations in Thailand, International journal of geoinformatics Vol. 9 (3): pp.69-77

López-Hoffman L., Anten N. P. R., Martínez-Ramos M. and Ackerly D. D. 2007. Salinity and light interactively affect neotropical mangrove seedlings at the leaf and whole plant levels, Oecologia 150: pp. 545-556

Lüttge U. 2008. Physiological Ecology of Tropical Plants, Springer, pp. 227-246

Mitra A. 2013. Sensitivity of Mangrove Ecosystem to Changing Climate, Springer

Nadezhdina N., Steppe K., De Pauw D. J. W., Bequet R., Čermak J. and Ceulemans R. 2009. Stem-mediated hydraulic redistribution in large roots on opposing sides of a Douglas-fir tree following localized irrigation, New Phytologist 184: pp. 932-943

Nadezhdina N., David T. S., David J. S., Ferreira M. I., Dohnal M., Tesař M., Gartner K., Leitgeb E., Nadezhdin V., Cermak J., Soledad Jimenez M. and Morales D. 2010. Trees never rest: the multiple facets of hydraulic redistribution, Ecohydrology 3: pp. 431-444

Nadezhdina N., and Vandegehuchte M. W. Steppe K. 2012. Sap flux density measurements based on the heat field deformation method, Trees 26: pp. 14391448

Nazim K., Ahmed M., Shahid Shaukat S., Uzair Khan M. and Muhammed Ali Q. 2013. Age and growth rate estimations of grey mangrove *Avicennia marina* (Forsk.) Vierh from Pakistan, Pakistan Journal of Botany 45 (2): pp. 535-542

Niglas A., Kupper P and Sellin A. 2014. Response of sap flow, leaf gas exchange and growth of hybrid aspen to elevated atmospheric humidity under field conditions, Annals of Botany, Oxford Journals: Open access - Research article

Nobel P. S. 2009. Physicochemical and environmental plant physiology, Fourth Edition, Elsevier Academic Press

Oliveira R. S., Dawson T. E. and Burgess S. S. O. 2005. Evidence for direct water absorption by the shoot of the desiccation-tolerant plant *Vellozia flavicans* in the savannas of central Brazil, Journal of Tropical Ecology 21: pp. 585-588

Oliveira R. S., Eller, C. B., Bittencourt P. R. L. and Mulligan M. 2014. The hydroclimatic and ecophysiological basis of cloud forest distributions under current and projected climates, Annals of Botany 113: pp. 909-920

Ong J.E. and Gong, W.K. 2013. Structure, Function and Management of Mangrove Ecosystems, ISME Mangrove Educational Book Series No. 2. International Society for Mangrove Ecosystems (ISME), Okinawa, Japan, and International Tropical Timber Organization (ITTO), Yokohama, Japan.

Paudel I., Naor A. and Cohen S. 2015. Simulating nectarine tree transpiration and dynamic water storage from responses of leaf conductance to light and sap flow to stem water potential and vapor pressure deficit, Tree Physiology 35(4): pp. 425-438

Pezeshki S. R. and De Laune R. D. 2012. Soil Oxidation-Reduction in Wetlands and its impact on plant functioning, MDPI, Biology 1: pp. 196-221

Philips. 2014. *http : //download.p4c.philips.com/l4b/9/928481600096_eu/928481600096−_eu_pss_nldbe.pdf* - Assessed 24 February 2015
http : //www.sapflowtool.com/SapFlowToolManual.html#SapFluxDensityModule - Accessed 24 November 2014

Polidoro B. A., Carpenter K. E., Collins L., Duke N. C., Ellison A. M., Ellison J. C., Farnsworth E. J., Fernando E. S., Kathiresan K., Koedam N. E., Livingstone S. R., Miyagi T., Moore G. E., Ngoc Nam V., Eong Ong J., Primavera J. H., Salmo S. G., Sanciangco J. C., Sukardjo S., Wang Y. and Wan Hong Yong J. 2010. The loss of Species: Mangrove extinction Risk and Geographic Areas of Global Concern, PLoS ONE 5(4)

Reef R. and Lovelock C. E. 2014. Regulation of water balance in mangroves, Annals of Botany

Robert E. M. R., Jambia A. H., Schmitz N., De Ryck D. J. R., De Mey J., Kairo J. G., Dahdouh-Guebas F., Beeckman H. and Koedman N. 2014. How to catch the patch? A dendrometer study of the radial increment through successive cambia in the mangrove *Avicennia*, Annals of Botany 113: pp. 741-752

Santina N. S., Reef R., Lockington D. A. and Lovelock C. E. The use of fresh and saline water sources by the mangrove *Avicennia marina*, Hydrobiologia 745: pp. 59-68

Schmitz N., Robert E. M. R., Verheyden A., Gitundu Kairo J., Beeckman H. and Koedam N. 2008. A patchy growth via successive and simultaneous cambia: key to success of the most widespread mangrove species *Avicennia marina*?, Annals of Botany 101: pp.49-58

Scholander P. F., Hammel H. T., Hemmingsen E. A. and Bradstreet E. D. 1964. Hydrostatic pressure and osmotic potential in leaves of mangroves and some other plants, Botany Vol. 52: pp. 119-125

Schwendenmann L., Dierick D., Köhler M. and Hölscher D. 2010. Can deuterium tracing be used for reliably estimating water use of tropical trees and bamboo?, Tree Physiology 30: pp. 886-900

Solartron metrology. 2015. Displacement sensors
http : //www.solartronmetrology.com/download.asbx?AttributeFileId = 324a6bf7 − c12f − 43b5 − acbd − fe616ac44d35 - Accessed 24 February 2015

Spalding M.D., Blasco F. and Field C.D. (Eds). 1997. World Mangrove Atlas, The International Society for Mangrove Ecosystems, Okinawa, Japan. 178 pp.

Steppe K. 2004. Diurnal dynamics of water flow through trees design and validation of a mathematical flow and storage model, Ghent University, PhD Thesis

Steppe K., De Pauw D. J. W., Leumeur R. and Vanrolleghem P. A. 2006. A mathematical model linking tree sap flow dynamics to daily stem diameter fluctuations and radial stem growth, Tree Physiology 26: pp. 257-273

Steppe K., Sterck F. and Deslauriers A. 2015a. Diel growth dynamics in tree stems: linking anatomy and ecophysiology, Trends in Plant Science (In Press)

Steppe K., Vandegehuchte M. W., Tognetti R. and Mencuccini M. 2015. Sap flow as a key trait in the understanding of plant hydraulic functioning, Tree Physiology 35: pp. 341-345

Suárez N., Sobrado M. A. and Medina E. 1998. Salinity effects on the leaf water relations components and ion accumulation patterns in *Avicennia germinans* (L.) L. seedlings, Oecologia 114: pp. 299-304

Taiz L. and Zeiger E. 2002. Plant physiology, third edition, Sinauer Associates

Tomlinson P. B. 1986. The botany of mangroves, Cambridge tropical biology series

Uddin S., Steppe K. and Vandegehuchte M. 2014. Canopy water uptake: an important survival mechanism of mangroves, Interuniversity program in physical land resources: Ghent University and VUB, Master Thesis

Vandegehuchte M. W. and Steppe K. 2012. Interpreting the Heat Field Deformation method: Erroneous use of thermal diffusivity and improved correlation between temperature ratio and sap flux density, Agricultural and Forest Meteorology 162 163: pp. 91 97

Vandegehuchte M. W. and Steppe K. 2013. Sap-flux density measurement methods: working principles and applicability, Functional Plant Biology 40(3): pp. 213-223

Vandegehuchte M. W., Guyot A., Hubeau M., De Swaef T., Lockington D. A. and Steppe K. 2014a. Modelling reveals endogenous osmotic adaptation of storage tissue water potential as an important driver determining different stem diameter variation patterns in the mangrove species *Avicennia marina* and *Rhizophora stylosa*, Annals of Botany 114(4): pp. 667-676

Vandegehuchte M. W., Guyot A., Hubeau M., De Groote S. R. E., De Baerdemaeker N. J. F., Hayes M., Welti N., Lovelock C. E., Lockington D. A. and Steppe K. 2014b. Long-term versus daily stem diameter variation in co-occuring mangrove species: Environmental versus ecophysiological drivers, Elsevier, Agricultural and Forest Meteorology 192-193: pp. 51-58

Van de Wal B. A. E., Guyot A., Lovelock C. E., Lockington D. A. and Steppe K. 2015. Influence of temporospatial variation in sap flux density on estimates of whole-tree water use in *Avicennia marina*, Trees 29: pp. 215-222

Wand'ondu V. W., Kairo J. G., Kinyamario J. I., Mwaura F. B. Bosire J. O., Dahdouh-Guebas F. and Koedam N. 2010 Phenology of *Avicennia marina* (Forsk.) Vierh. in a Disjunctly-zoned Mangrove Stand in Kenya, Western Indian Ocean J. Mar. Sci. Vol. 9 (2): pp. 135-144

West. A. G., Patrickson S. J. and Ehleringer J. R. 2006. Water extraction times for plant and soil materials used in stable isotope analysis, Rapid communications in mass spectrometry (20): pp. 1317-1321

Zimmerman D., Westhoff M., Zimmerman G., Geβner P., Gessner A., Wegner L. H., Rokitta M., Ache P., Schneider H., Vásquez J. A., Kruck W., Shirley S., Jakob P., Hedrich R., Bentrup F.-W., Bamberg E. and Zimmermann U. 2007. Foliar water supply of tall trees: evidence for mucilage-facilitated moisture uptake from the atmosphere and the impact on pressure bomb measurements, Protoplasma 232: pp. 11-34

Appendix

A. Personal communication with professor Jean W. H. Yong, Singapore University of Technology and Design - 18 July 2014 and 18 November 2014

Question For some greenhouse experiments I would like to grow *Avicennia marina*. I know this species tolerates considerable variations of water salinity, extreme conditions of temperature as well as long submergence of its pneumatophores during exceptional floods. But can you help me to create a good stable starting environment for my experiments?

> **Reply** *For Avicennia marina, we found that planting them, "half-way" into the moist soil (Figure 5.1), gave the best results. From our lab experiences, it is important to keep the soil moist (use a basin to soak).*

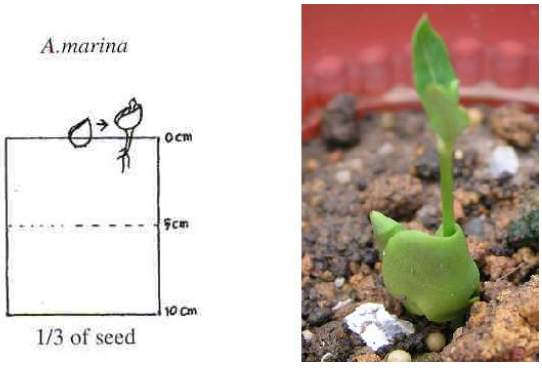

Figure 5.1: Planting *Avicennia marina*. Left: Schematic. Right: Practice.

B. Calibration of the mini HFD-sensor

Due to technical problems the calibration was only performed for positive water flows for 3 out of 4 mini HFD-sensors (1 sensor broke down after the experiments). The performed calibrations were compared to two conversion possibilities. In 2 out of 3 calculations the classical calculation of the HFD-ratio ($RSF = (dT0_{s-a} + dT_{s-a}).(dT_{as})^{-1}$) had a lesser fit. As such, it should be considered to alter the calibration procedure. By removing the K-value ($= dT0_{s-a}$) in the calculations a better fit was obtained ($RSF_s = (dT_{s-a})(dT_{as})^{-1}$). RSF_s had the best fit for 2 out of 3 calibrations. Additionally, for the calibration where RSF out-competed RSF_s, only a small difference was detected. It could be considered to extrapolate the obtained calibration for positive water flows to negative water flows. This is theoretically possible in the case of a perfect sensor (T1 and T2 at equal distances of the heater), however, in practice, this is rarely the case. Nonetheless, this method may give a good indication of the magnitude of the negative flows. By this, the calibration time can be halved and multiple samples can be calibrated in a shorter time span. In this research this would have been beneficial as 4 samples had to be calibrated as quick as possible after the deuterium experiment in order to avoid dehydration, fungus growth and approach in vivo conditions as closely as possible. However, only one calibration could be done at the time with an average duration of 9-12 hours per calibration of either a positive or a negative water flow.

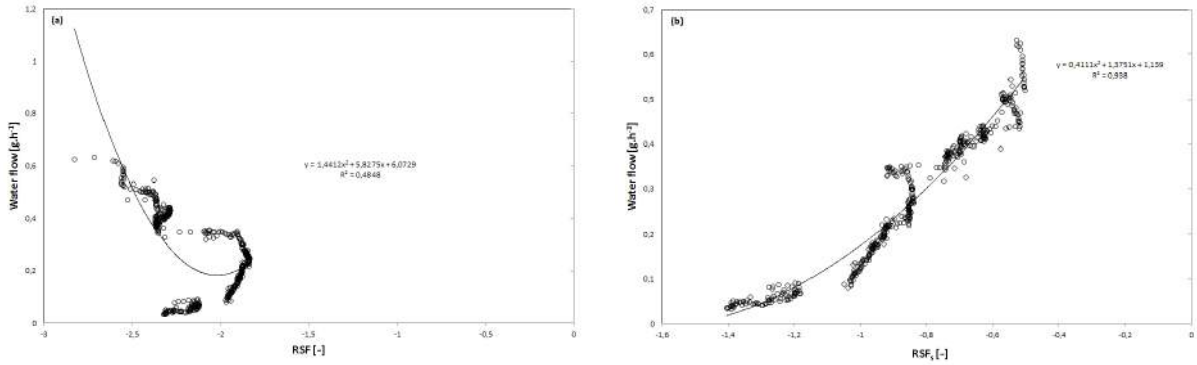

Figure 5.2: The HFD-ratio as a function of water flow of mini HFD-sensor 1. (a) $RSF = (dT0_{s-a} + dT_{s-a}).(dT_{as})^{-1}$. (b) $RSF_s = (dT_{s-a})(dT_{as})^{-1}$.

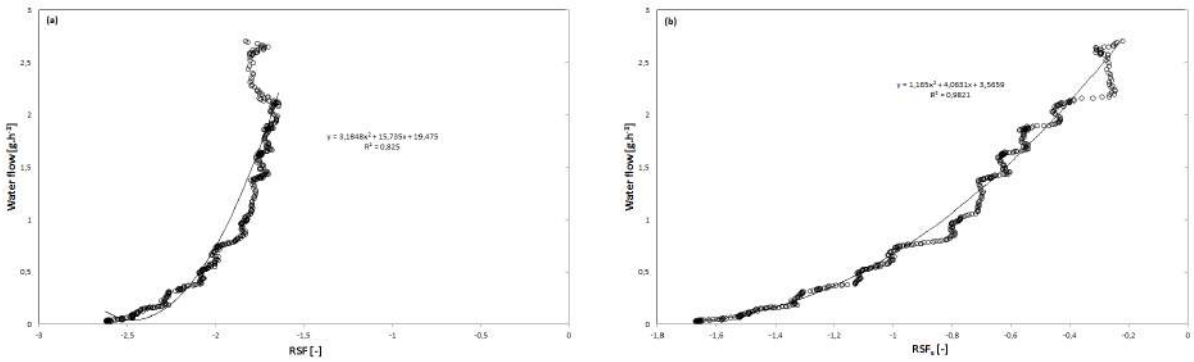

Figure 5.3: The HFD-ratio as a function of water flow of mini HFD-sensor 2. (a) $RSF = (dT0_{s-a} + dT_{s-a}).(dT_{as})^{-1}$. (b) $RSF_s = (dT_{s-a})(dT_{as})^{-1}$.

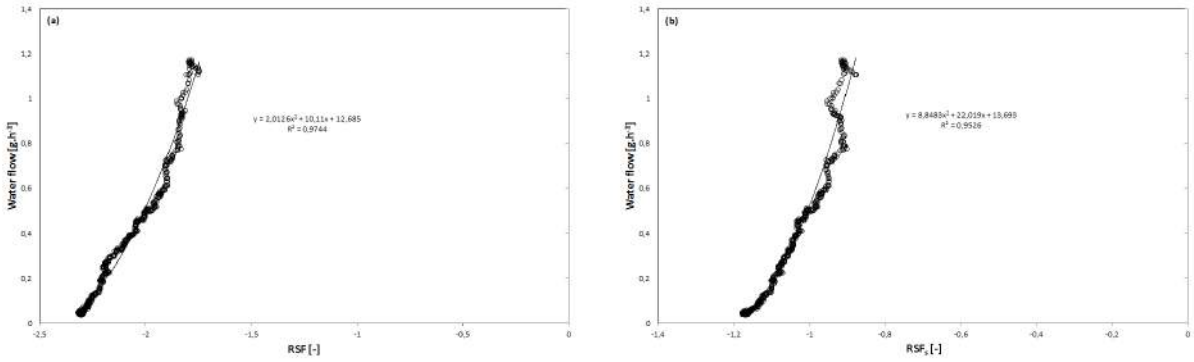

Figure 5.4: The HFD-ratio as a function of water flow of mini HFD-sensor 3. (a) $RSF = (dT0_{s-a} + dT_{s-a}).(dT_{as})^{-1}$. (b) $RSF_s = (dT_{s-a})(dT_{as})^{-1}$.